Chapter 3

(PNP)$CrPh_3$ and (PNP)$CrPh_2Cl$ Complexes as Well-Defined Ethylene Trimerization Catalysts: Insights into Mechanism and Active Species

Part of the text of this chapter has been published previously:

Agapie, T.; Schofer, S. J.; Labinger, J. A.; Bercaw, J. E. *J. Am. Chem. Soc.* **2004**, *126*, 1304.

Abstract

In order to study the factors that affect the unprecedented activity and selectivity of the chromium-based ethylene trimerization catalyst involving the diphosphine ligand (*o*-CH_3O-C_6H_4)$_2$PN(Me)P(*o*- CH_3O-C_6H_4)$_2$ (PNP^{OMe} (**1**)) reported by bp, we have synthesized complexes of the general type (PNP)$CrPh_3$ ((PNP^{OMe}-d_{12})$CrPh_3$ (**11**) and (PNP^{SMe}-d_{12})$CrPh_3$, (**12**)) and (PNP^{OMe}-d_{12})$CrPh_2Cl$ (**14**) containing deuterated methoxy or thioether groups. The solid state structures of these complexes display octahedral geometries with coordination of PNP ligands in a (P,P,O)-κ^3 or (S,P,S)-κ^3 fashion. Dynamic processes occur in solution at room temperature to render all four of the deuterated methoxy or thioether groups equivalent on the ^{2}H NMR timescale; two distinct coalescence processes are observed by variable temperature ^{2}H NMR spectroscopy for all species examined. The neutral species **11** and **14** react with ethylene by insertion into chromium-phenyl bonds, but 1-hexene is not observed under these conditions. Activation of **11** by protonation with $H^+(OEt_2)_2B[C_6H_3(CF_3)_2]_4^-$ and activation of **14** by halide abstraction with $Na^+B[C_6H_3(CF_3)_2]_4^-$ in the presence of ethylene provide active trimerization catalysts that give similar selectivity to 1-hexene as the originally reported system. These complexes represent the first examples of active, well-defined, homogeneous trimerization catalysts based on chromium. Both the model systems and our attempts to reproduce the original bp system provide catalysts that decompose via a process that is first-order in chromium. Our catalysts display activity on the same order of magnitude as the original system when they are activated in the presence of 900 equivalents of diethyl ether. Trimerization of a 1:1 mixture of C_2H_4 and C_2D_4 gives only C_6D_{12}, $C_6D_8H_4$, $C_6D_4H_8$, and C_6H_{12}, the 1-hexene isotopomers without H/D scrambling, which is consistent with a trimerization mechanism involving metallacyclic intermediates. Activated complexes **11** and **14** initiate trimerization primarily through ethylene insertion into chromium-phenyl bond, followed by β-hydrogen elimination and reductive elimination to give the active species, rather than via reductive elimination of biphenyl.

Introduction

The transition metal catalyzed oligomerization of ethylene typically produces a broad range of α-olefins.[1] Distillation is required to isolate pure samples of desired α-olefins. Linear α-olefins, especially 1-hexene and 1-octene, are important comonomers for the production of linear low-density polyethylene.[2] In 1989 Briggs reported the chromium-catalyzed selective trimerization of ethylene to produce 1-hexene.[3] Several recent reports describe other chromium-based catalysts that can carry out this process with high selectivity.[4] Some examples of these catalysts are shown in Figure 1. Catalysts based on titanium,[5] tantalum,[6] and vanadium[7] complexes have also been found to have application in this area.

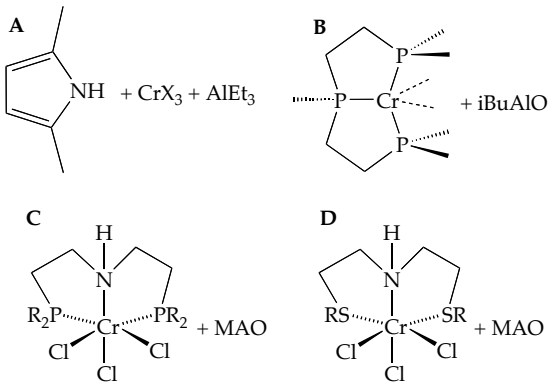

Figure 1. Examples of chromium-based ethylene trimerization catalysts. A. Phillips' chromium/pyrrole catalyst.[4b] B. Albemarle's chromium/Triphos catalyst.[4e] C. Sasol's chromium/P_2NH catalyst.[4c] D. Sasol's chromium/S_2NH catalyst.[4d]

The most active and selective of the chromium-based ethylene trimerization catalysts was reported by bp (formerly British Petroleum) in 2002 and involves a Cr(III) precursor,[8] a diphosphine ligand ((*o*-MeO-$C_6H_4)_2PN(Me)P(o$-MeO-$C_6H_4)_2$, PNP^{OMe} (**1**)), and activation by methylaluminoxane (MAO) (Scheme 1).[9] This catalyst produces 1-hexene with approximately 2 X 10^6 turnovers per hour and gives 90.0% selectivity to C_6 products and 99.9% selectivity for 1-hexene within the C_6 fraction. bp

reports that catalyst activity remains constant over the course of hours. A comparison of the activity and selectivity of the bp system with other reported chromium-based ethylene trimerization catalysts is shown in Table 1.

Scheme 1.

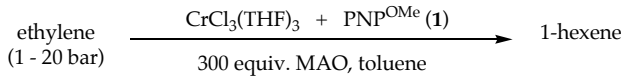

	Cr/pyrrole (Phillips)	**Cr/Triphos** (Albemarle)	**Cr/P_2NH** (Sasol)	**Cr/S_2NH** (Sasol)	**Cr/PNP** (bp)
Productivity (g/gCr.h)	100,000 (at 54 bar)	17,000 (at 50 bar)	37,400 (at 40 bar)	160,840 (at 30 bar)	1,033,000 (at 20 bar)
Selectivity to C_6 (%)			94	98.4	90.0
Purity of 1-hexene (%)	99.0	99.0	99.1	99.7	99.9

Table 1. Comparison of activity and selectivity for chromium-based ethylene trimerization catalysts.

Variations of the diphosphine ligand have been shown to have a dramatic effect on trimerization activity, as shown in Figure 2. In the original report, both the *ortho*-methoxy group on the aryl ring and the methyl amine in the backbone were critical for catalyst activity. Replacing the *ortho*-methoxy group (**1**, **4**, **5**) with a sterically similar ethyl group (**2**) or a hydrogen (**3**) renders the system inactive towards ethylene consumption, as does replacement of the methyl amine backbone with either a methylene (**6**) or ethylene (**7**) linker. However, the bp report does not describe the isolation of discrete chromium complexes that act as catalyst precursors, and the reasons behind the dependence of trimerization activity on ligand variations are not understood. In fact, recent results in our laboratory have shown that a chromium complex of ligand **6** is slightly active for ethylene trimerization.[10]

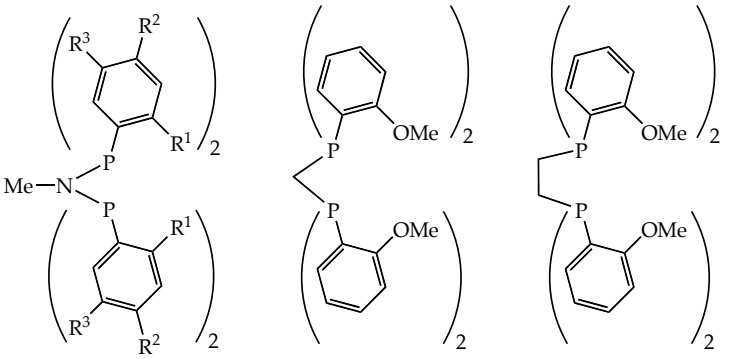

*1: R^1 = OMe, R^2 = R^3 = H
2: R^1 = Et, R^2 = R^3 = H
3: R^1 = R^3 = H, R^2 = OMe
*4: R^1 = R^3 = OMe, R^2 = H
*5: R^1 = OMe, R^2 = H, R^3 = F
* = active for trimerization

6

7

Figure 2. Diphosphine ligands examined by bp for ethylene trimerization activity when combined with $CrCl_3(THF)_3$ and activated with MAO in toluene.

A general mechanism has been proposed to explain the selectivity for 1-hexene in these systems.[3] This mechanism is shown in Scheme 2, and its key features include metallacyclic intermediates and a Cr^n/Cr^{n+2} redox couple. The mechanism involves initial coordination and oxidative coupling of 2 equivalents of ethylene to Cr^n to form a chromacyclopentane of oxidation state Cr^{n+2}. This species may then coordinate and insert another equivalent of ethylene to form a chromacycloheptane or undergo β-hydrogen elimination. While the chromacyclopentane is too rigid to undergo β-hydrogen elimination, the chromacycloheptane is flexible enough to do so. The resulting chromium alkenyl hydride species can then react via reductive elimination to form 1-hexene and Cr^n to turn over the catalytic cycle. The observed high selectivity for 1-hexene indicates that insertion of 1-hexene into the chromium-hydride bond of the hydride species is not fast enough to compete with reductive elimination. A DFT study on the mechanism of chromium-catalyzed formation of 1-hexene involving metallacyclic intermediates was recently reported.[11]

Scheme 2.

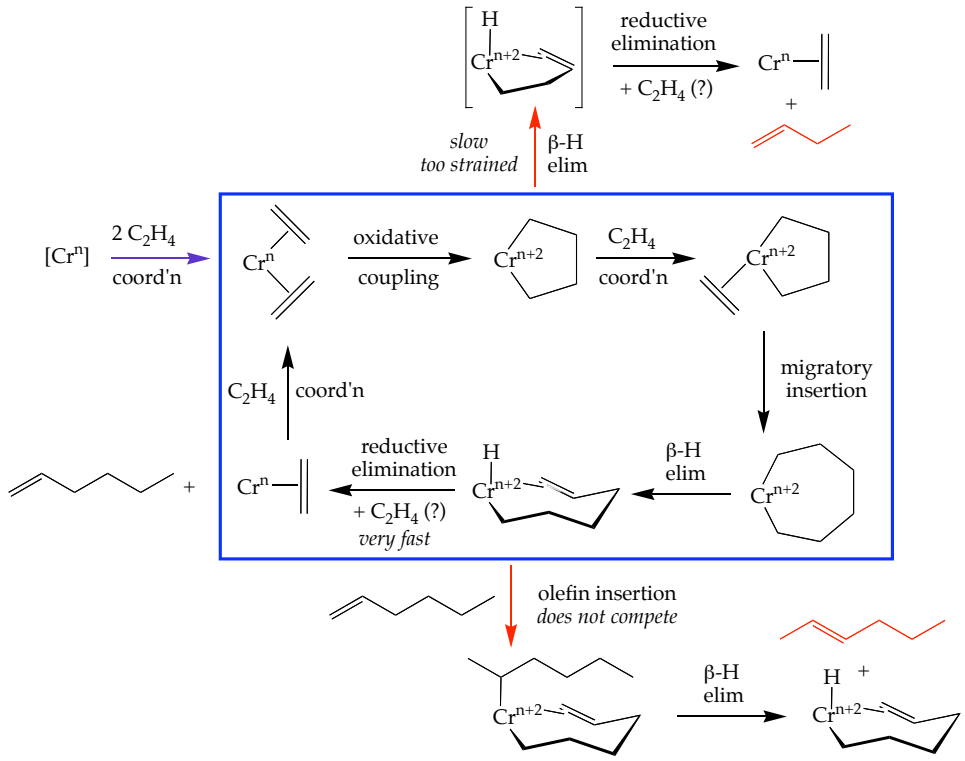

To date there is little experimental evidence to support the proposed mechanism. This mechanism is consistent with studies of metallacyclic derivatives of platinum, which have demonstrated that platinacyclopentanes are more stable to decomposition via β-hydrogen elimination than platinacycloheptanes.[12] However, prior to this work, there had only been one experimental study on chromium to support this proposed mechanism. This study involves a comparison of the decomposition temperatures of the chromacyclopentane complexes $Cp^*(PR_3)Cr(CH_2(CH_2)_2CH_2)$ ($Cp^* = \eta^5\text{-}C_5Me_5$; R = Me, Et) and $(Me_2NC_2H_4C_5Me_4)Cr(CH_2(CH_2)_2CH_2)$ with the decomposition temperatures of the analogous chromacycloheptane complexes.[13] The authors find that the chromacyclopentane complexes decompose to give 1-butene at higher temperatures than the chromacycloheptane complexes decompose to give 1-hexene. In the case of the $[(Me_2NC_2H_4C_5Me_4)Cr]$ complexes the decomposition temperatures differ by approximately 100 °C. However, these model complexes are not active for the trimerization of ethylene.

In an effort to learn more about the chromium-based catalytic system reported by bp, we began to investigate the synthesis, characterization, and reactivity of [(PNP)Cr] complexes. Well-defined [(PNP)Cr] complexes that can be activated stoichiometrically to catalyze ethylene trimerization have been prepared, and the selectivities and activities of these catalysts have been compared to the originally reported bp system. Work has been directed at gaining insight into the nature of the active chromium complexes and intermediates, including the oxidation states of chromium, the structures of the active catalyst and relevant intermediates, and the essential features of the PNP ligand. Using these well-defined complexes we have studied the mechanism of 1-hexene formation and examined the initiation mechanism for these catalysts. With an understanding of the catalyst mechanism, we hope to improve activity and selectivity, as well as to design catalysts for more valuable products such as 1-octene.

Results and Discussion

To address the issues described above, we selected complexes of the general form (PNP)CrR_3 and (PNP)CrR_2X (R = carbyl; X = halide) as catalyst precursors. These types of complexes may be activated stoichiometrically in the presence of ethylene to form active trimerization catalysts. In the case of the tricarbyl complex, activation may proceed via protonation of one of the carbyl groups, while in the case of the dicarbyl halide complex, activation should be possible by abstraction of a halide. In both cases activation generates a cationic dicarbyl chromium complex of the form $[(PNP)CrR_2]^+$, which may react with ethylene to lose R_2 and generate $[(PNP)Cr]^+$ ($[Cr^n]$ in Scheme 2), which can enter the catalytic cycle. These activation routes are shown in Scheme 3.

Scheme 3.

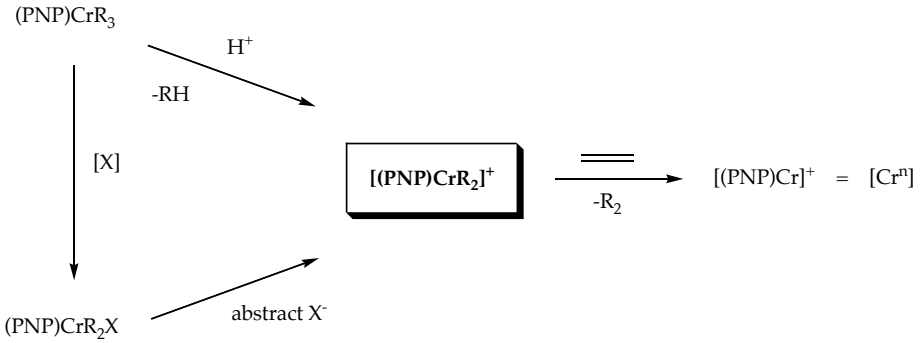

We have chosen $CrPh_3(THF)_3$ (**8**) as the chromium tricarbyl starting material. This complex is one of few known Cr(III) tricarbyl complexes; its synthesis from $CrCl_3$ and PhMgBr in THF was originally reported in 1959,[14] and its crystal structure was reported in 1983.[15] Compound **8** is very unstable to reductive elimination of biphenyl at temperatures above –30 °C or in the absence of THF, and it is difficult to separate from magnesium halides which co-crystallize with the complex during purification. However, **8** can be isolated as red crystals by repeated recrystallization from THF and stored at low temperature for months.

Synthesis and Characterization of PNP Ligands

Because our target chromium complexes were paramagnetic Cr(III) species, we have designed PNP ligands that are selectively deuterated for the purpose of examining these complexes by ^{2}H NMR spectroscopy. While the ^{1}H signals for paramagnetic complexes are often broadened and shifted due to rapid spin relaxation, it is known that the linewidths of ^{2}H NMR spectra are approximately 40 times narrower than the corresponding ^{1}H signals, and the overall resolution of ^{2}H spectra may be better than ^{1}H spectra by almost 7 times.[16] This effect has been observed to be especially true for Cr(III) complexes.[16]

A deuterated methoxy substituent was installed on the aryl ring of the ligand (PNP^{OMe}-d_{12}, **9**). We also synthesized the analogous ligand containing a

thioether in place of the ether of the parent ligand (PNP^{SMe}-d_{12}, **10**). Synthesis of **9** and **10** may be accomplished by either a stepwise (Scheme 4) or a convergent route (Scheme 5).[17] Although the stepwise route often gives overall yields as high as 60-70%, it is somewhat irreproducible. The convergent route provides a more reliable way to synthesize desired ligands. In fact, all attempts to synthesize **10** via the stepwise route have been unsuccessful. Additionally, the convergent route offers convenient access to a variety of ligands, as the individual building blocks can be combined to make a range of novel ligands.

Scheme 4.

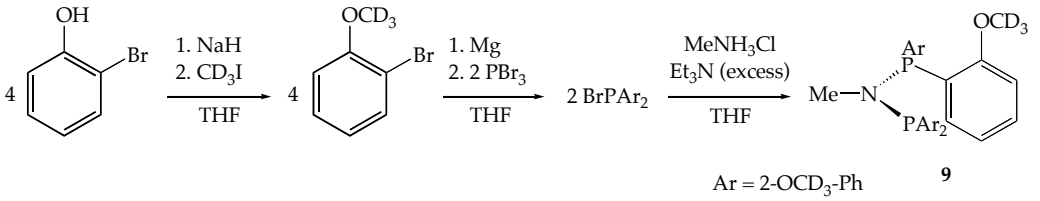

The deuterated methyl group may be installed by deprotonation of the corresponding 2-bromophenol or –thiophenol, followed by reaction with CD_3I. For the stepwise route, *in situ* preparation of the aryl Grignard reagents, followed by reaction with 0.5 equivalents of PBr_3 generates the diaryl phosphorus bromide in greater than 90% yield, according to the ^{31}P NMR spectrum of an aliquot of this reaction. The diaryl phosphorus bromide may then be reacted with 0.25 equivalents of $MeNH_3Cl$ in the presence of excess tertiary amine to form the desired ligand. For the convergent route, the aryl Grignard may be reacted with 0.25 equivalents of $(Me)N(PCl_2)_2$, which can be prepared according to literature methods.[18] The progress of these reactions can be conveniently monitored by ^{31}P NMR spectroscopy. The room temperature ^{31}P NMR spectra of **9** and **10** show characteristic resonances at $\delta = 54$ ppm and $\delta = 50$ ppm in THF, respectively. The room temperature ^{2}H spectra of **9** and **10** show characteristic resonances at $\delta = 3.60$ ppm and $\delta = 2.26$ ppm in dichloromethane, respectively.

Scheme 5.

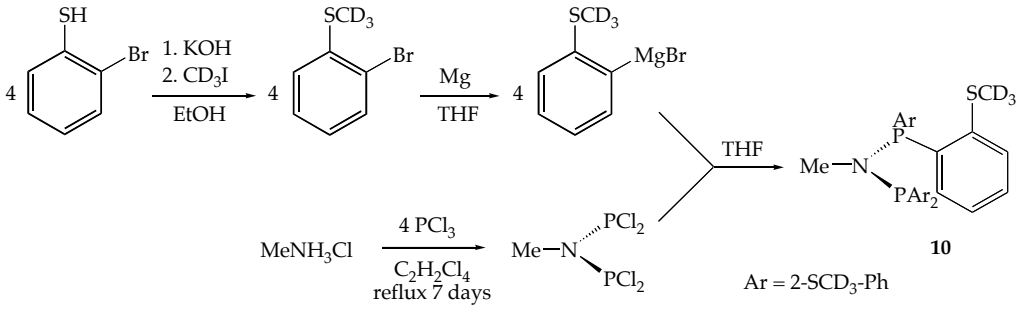

Synthesis and Characterization of Chromium Triphenyl Complexes

Synthesis and Characterization of (PNP^{OMe}-d_{12})CrPh$_3$

Reaction of the diphosphine ligands **9** and **10** with $CrPh_3(THF)_3$ (**8**) in dichloromethane gives high yield of the desired (PNP)$CrPh_3$ complexes. Ligand **9** reacts with **8** to form (PNP^{OMe}-d_{12})$CrPh_3$ (**11**) as a red, microcrystalline solid in 68% yield, as shown in Scheme 6. Slow diffusion of petroleum ether into a dichloromethane solution of **11** at –35 °C provides crystals suitable for structural determination by X-ray diffraction. The solid state structure of **11** shows the presence of two distinct molecules of **11** in the unit cell; one of them is shown in Figure 3. The structure reveals that the chromium is hexacoordinate with the PNP^{OMe} ligand coordinated to chromium in a (P,P,O)-κ^3 mode. The chromium-oxygen bond lengths of 2.279(3) Å and 2.293(2) Å are similar to other chromium-oxygen bonds that are *trans* to a phenyl group.[15] The structure also indicates that coordination of methoxy to chromium shortens the chromium-phosphorus bond distance of the chelating phosphorus by 0.11 Å to 0.17 Å, from 2.6164(12) Å to 2.5044(12) Å and from 2.6597(12) Å to 2.4897(11) Å. The nitrogen in the structure is pyramidal, indicating the absence of multiple bonding between the nitrogen and phosphorus atoms in the solid state.

Scheme 6.

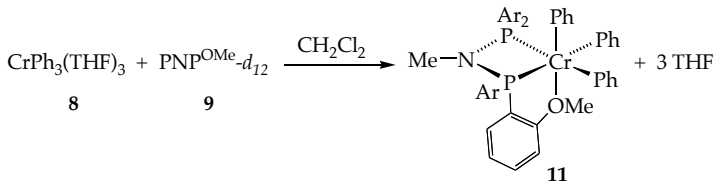

8 9 11

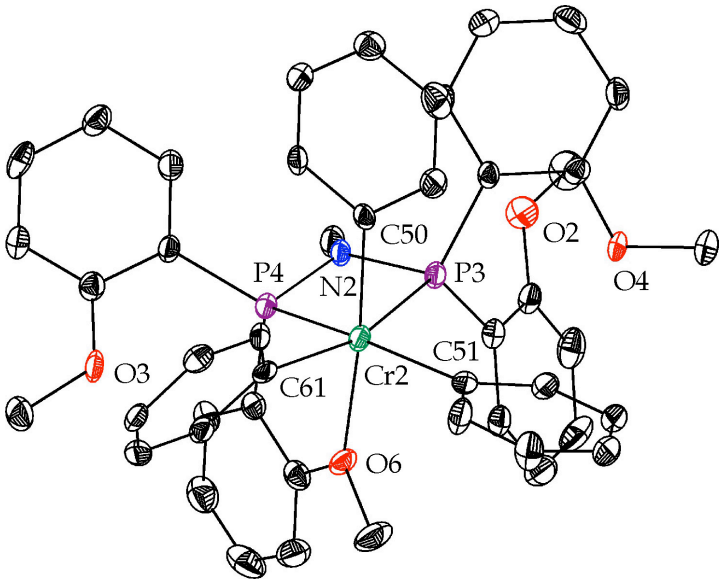

Figure 3. Molecular structure of **11** with 50% probability ellipsoids.

Although the solid state structure of **11** indicates the coordination of a single methoxy group from the ligand to chromium, the room temperature ^{2}H NMR spectrum of this complex in dichloromethane displays only a single peak at δ = 8.47 ppm. The observation of a single peak at room temperature suggests that a dynamic process occurs in solution to render all four of the methoxy groups equivalent on the NMR time scale. In fact, variable temperature ^{2}H NMR spectra of **11** show two distinct coalescence points, as shown in Figure 4.

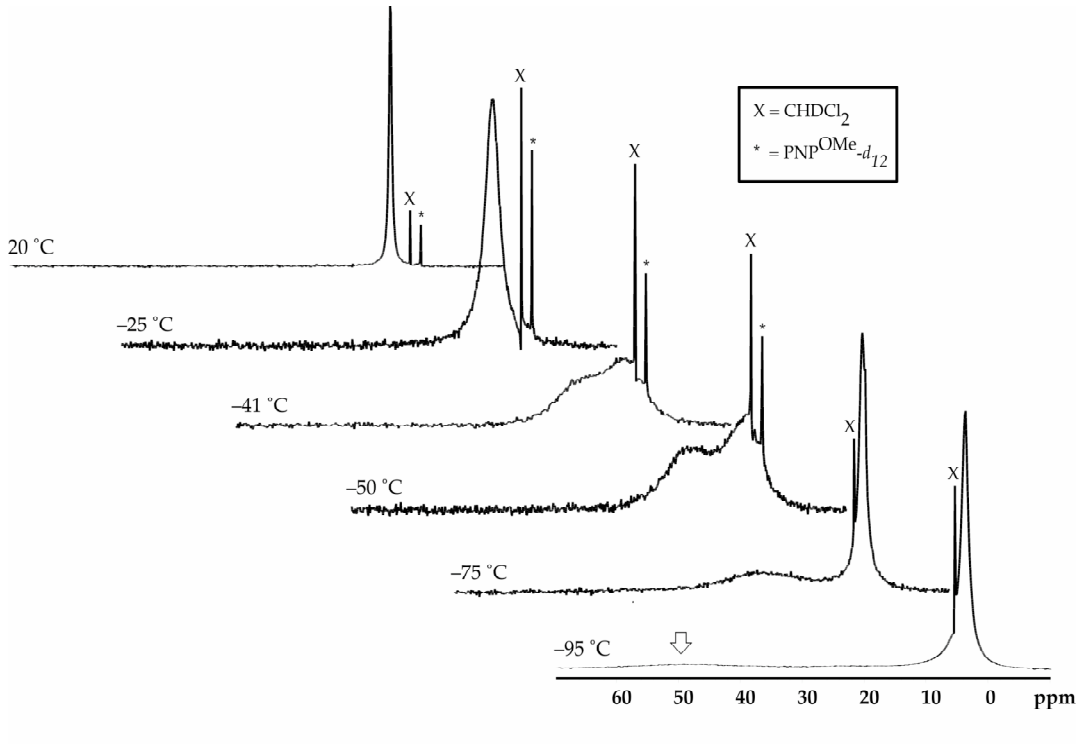

Figure 4. Variable temperature ^{2}H NMR spectra of **11** in dichloromethane.

The peaks in the spectra may be assigned as either free or chromium-bound methoxy groups. At –95 °C it is possible to slow the exchange processes enough to observe the static structure of **11**, which has only one methoxy group coordinated to chromium. We observe a very broad peak centered at δ = 50 ppm, which we have assigned to the methoxy group bound to chromium. The three non-coordinated methoxy groups appear as a single peak in the diamagnetic region (δ ≈ 4 ppm). As the sample is warmed a coalescence point is observed at –75 °C, and at –50 °C we observe two peaks in a 1:1 ratio. Finally, as the solution is warmed further, the complex undergoes another coalescence point at –41 °C, until, at about –25 °C and above, only one peak is observed for all four of the exchanging methoxy groups. This process is fully reversible.

We propose the occurrence of two separate exchange processes for complex **11** (Figure 5). The exchange process that occurs at –75 °C and above involves the dissociation of a methoxy chelated to one phosphorus, followed

by recoordination of a methoxy group from the other phosphorus. This process occurs on the same hemisphere of the complex. We assign the downfield peak in the –75 °C spectrum to the two methoxy groups that are exchanging for coordination to chromium and the upfield peak to the two methoxy groups on the other side of the molecule. The process that occurs at –41 °C and above involves dissociation of a methoxy group from one hemisphere of the complex, followed by a Berry pseudorotation and recoordination of a methoxy group from the other hemisphere. Although we have determined the temperatures at which these processes occur, quantitative thermodynamic parameters have not been determined for these exchange processes due to paramagnetic broadening and variation of chemical shift with temperature.[19] We believe that the labile coordination of oxygen to chromium is key to the remarkable activity and selectivity of this catalyst.

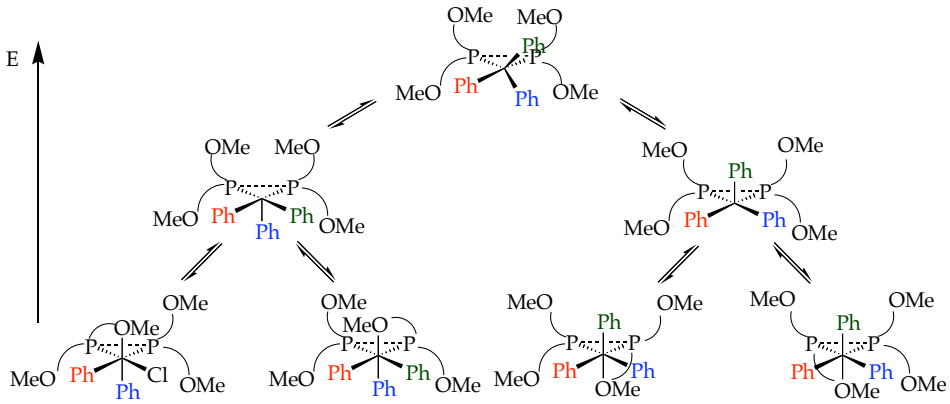

Figure 5. Proposed exchange processes to explain the observed variable temperature ^{2}H NMR spectra of **11**.

We can determine the spin state for chromium complex **11**. The EPR spectrum of **11** at 20 K in a toluene glass consistent with Cr(III) species with three unpaired electrons and $S = 3/2$ (Figure 6).[20] Evans method determination of the solution magnetic susceptibility[21] indicates an effective magnetic moment (μ_{eff}) of 3.8 BM in dichloromethane, which is consistent with a quartet ground state and the presence of three unpaired electrons.

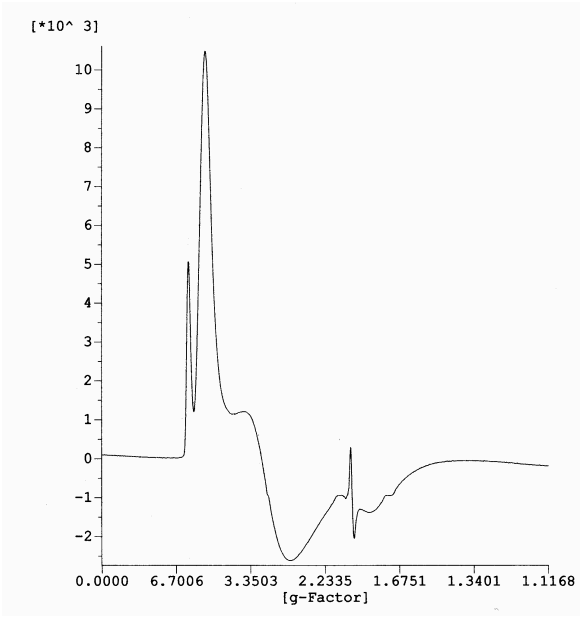

Figure 6. EPR spectrum of a glassy toluene solution of **11** at 20 K.

Synthesis and Characterization of (PNP^{SMe}-d_{12})CrPh$_3$

Ligand **10** reacts with **8** to form (PNP^{SMe}-d_{12})CrPh$_3$ (**12**) as a brown powder in 56% yield, as shown in Scheme 7. Slow diffusion of petroleum ether into a dichloromethane solution of **12** at –35 °C provides crystals suitable for analysis by X-ray diffraction. The solid state structure of **12** is shown in Figure 7. This complex shows a different binding mode for the PNP ligand; it displays coordination of two sulfurs and one phosphorus to chromium in a (S,P,S)-κ^3 mode. Unfortunately, these crystals were suitable only for determination of connectivity in this structure, and actual bond lengths have not been obtained for this complex. The more favorable binding of sulfur than phosphorus to the chromium triphenyl moiety suggests that this chromium center is relatively soft. It is interesting to compare the binding mode observed for **12** with the binding modes observed for two novel (PNP)CrCl$_3$ complexes prepared by Theodor Agapie.[22] In (PNP^{NMe2}-d_{24})CrCl$_3$ the ligand binds in a (N,P,N)-κ^3 mode, and in [(PNP$^{NMe2(OMe)3}$-d_{15})CrCl$_3$]$_2$ the ligand binds in a (N,P)- κ^2 mode, and the complex forms a chloride-bridged dimer, suggesting that the chromium center in the

trichloride is harder than in the triphenyl, as it prefers to bind nitrogen rather than either phosphorus or oxygen. However, the observed structural data does not provide insight into the role of geometric parameters, such as carbon-sulfur or carbon-nitrogen bond lengths, in determining the diverse binding modes for these ligands to chromium.

Scheme 7.

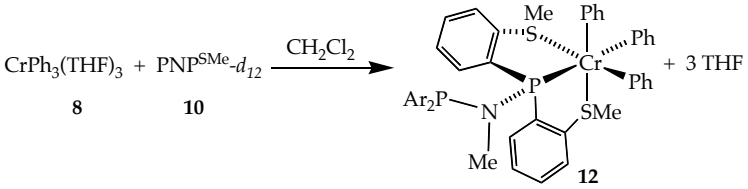

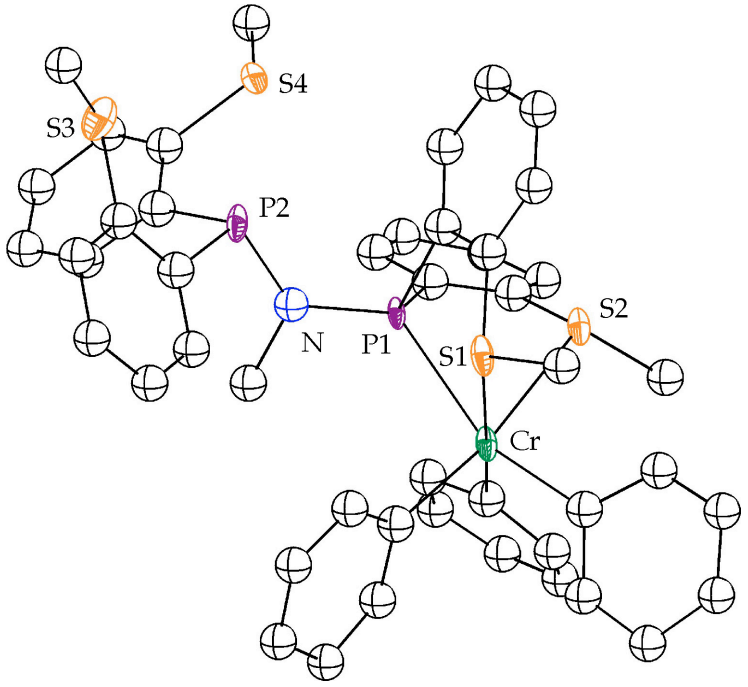

Figure 7. Molecular structure of **12**. Heteratoms have been refined anisotropically and are displayed with 50% probability ellipsoids. All carbons were refined isotropically.

The room temperature ^{2}H NMR spectrum of **12** in dichloromethane displays a single peak at δ = -3.8 ppm. As for **11**, the observation of a single peak in the room temperature ^{2}H NMR spectrum is indicative of the occurrence of exchange processes. An examination of the ^{2}H NMR spectra of

this compound at –100 °C shows a very broad peak centered at δ = -38 ppm, as well as a peak upfield at δ = 2.52 ppm. The relative integrations of the downfield peak as compared to the peak in the diamagnetic region suggest that the static structure of **12** in solution involves coordination of a single thioether group to chromium. Variable temperature ^{2}H NMR spectra of this compound show two distinct coalescence points, one at –85 °C and the other at 5 °C, as shown in Figure 8. We propose two separate exchange processes analogous to those suggested for **11**, to explain these data. Although the solid state structure of **12** involves a phosphine coordinated to chromium and the other phosphine further away from the paramagnetic chromium center, we do not observe a ^{31}P signal for this complex, even at –95 °C.

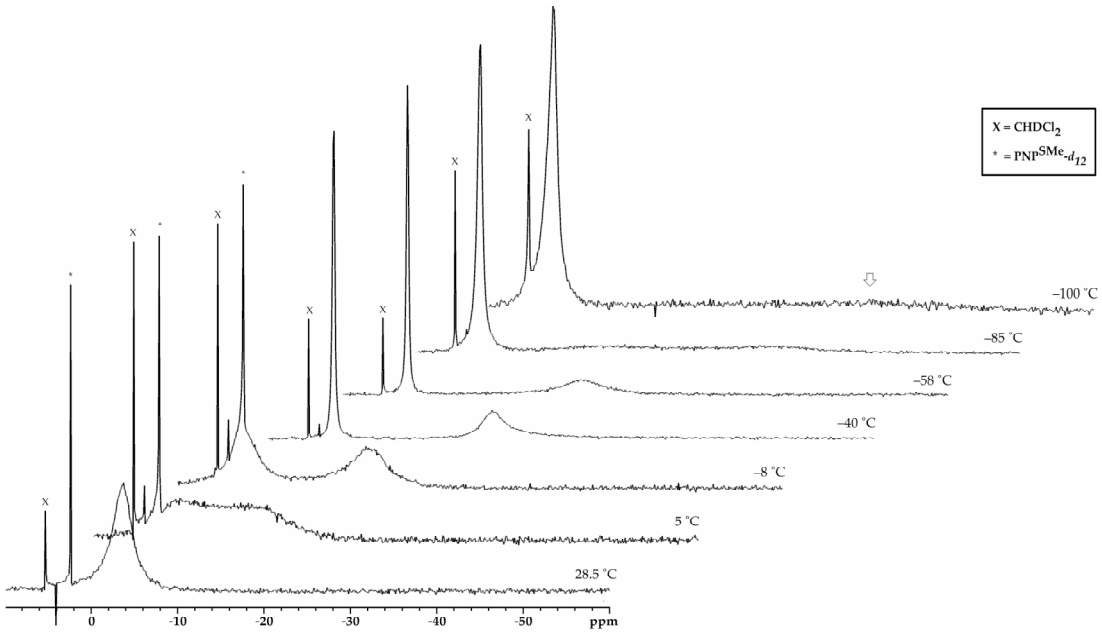

Figure 8. Variable temperature ^{2}H NMR spectra of **12** in dichloromethane.

The spin state for **12** has been determined by EPR at 20 K in a toluene glass, as shown in Figure 9. This spectrum is consistent with a Cr(III) species with a quartet ground state and $S = 3/2$.[20]

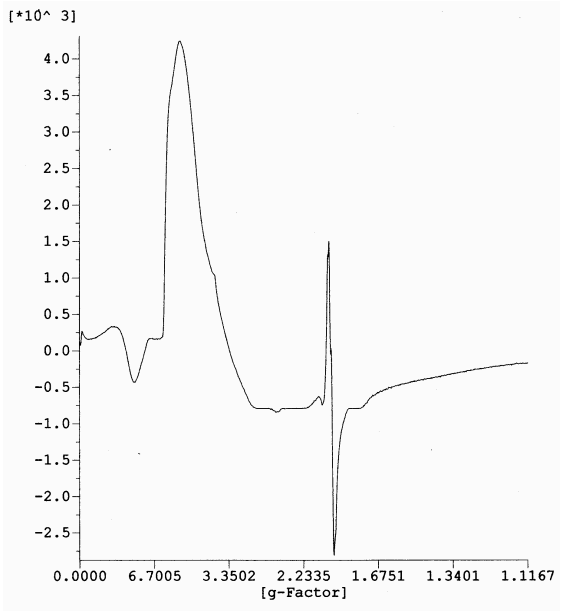

Figure 9. EPR spectrum of a glassy toluene solution of **12** at 20 K.

Synthesis and Characterization of Chromium Diphenyl Halide Complexes

Isolation of (PNP^{OMe}-d_{12})$CrPh_2X$ (X = Cl, Br) Complexes

It is possible to isolate complexes of the general form [(PNP^{OMe}-d_{12})$CrPh_2X$] by a variety of routes. Specifically, (PNP^{OMe}-d_{12})$CrPh_2X$ (X = Cl, Br (**13**)) has been isolated as a decomposition product of **11** in dichloromethane in the presence of magnesium halides that remain from the synthesis of **8** from PhMgBr and $CrCl_3$. This complex was originally isolated as two different mixtures of the chloride and bromide complexes (**13a** and **13b**). Dichloromethane solutions of **11** undergo halogenation, which seems to be catalyzed by light and the presence of added $MgBr_2$ and is proposed to occur via a mechanism involving radicals, as shown in Scheme 8. The proposed mechanism involves initial coordination of MgX_2 to the methoxy group coordinated to chromium, followed by coordination of a lone pair from a chloride on dichloromethane to chromium. The carbon-chloride bond of dichloromethane can then undergo homolytic cleavage and abstract Ph• from chromium to give CH_2PhCl and (PNP^{OMe}-d_{12})$CrPh_2Cl$ (**14**). This complex may

undergo halide exchange to yield a product that is a mixture of the chloride and bromide complex.

Scheme 8.

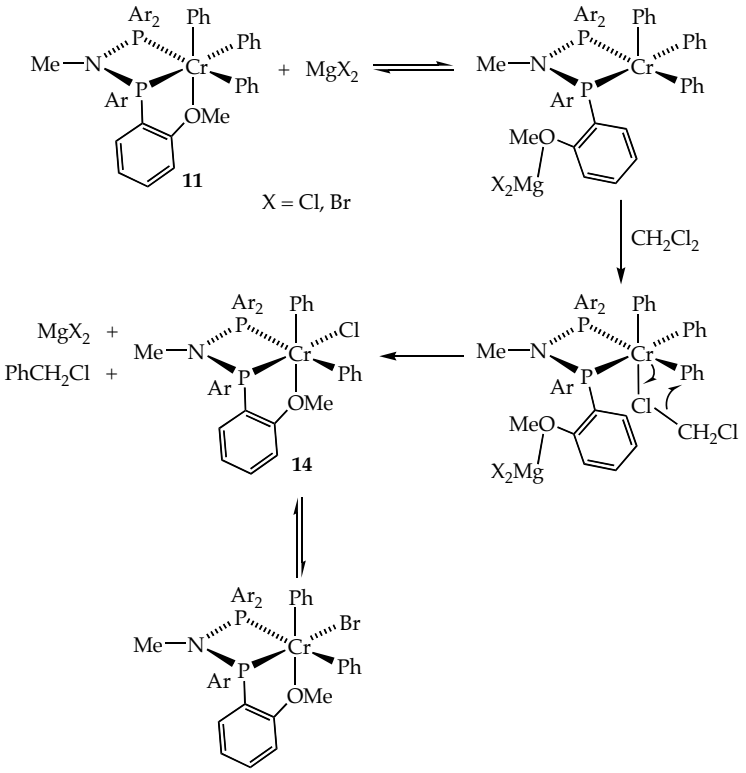

Slow diffusion of petroleum ether into dichloromethane solutions of **13a** or **13b** at –35 °C provides X-ray quality crystals. The solid state structures of mixtures of **13a** and **13b** have been determined by X-ray crystallography and show variable chromium-oxygen bond lengths. The structure of **13b** is shown in Figure 10. Complex **13a** crystallized as a mixture with the halide site occupied by chloride 76% of the time and bromide 24% of the time. The halide site in **13b** is occupied by bromide 81% of the time and chloride 19% of the time. The structures both display (P,P,O)-κ^3 coorindation around chromium, and in **13a** the phosphorus chelated to the methoxy group is closer to chromium by 0.19 Å. The halide is *trans* to the chelated phosphorus. Presumably the phenyl groups prefer to be *trans* to the methoxy group rather than to phosphorus because of the weaker *trans* influence of the ether ligand. Additionally the phenyl groups prefer to be *trans* to the phosphorus that is bound more loosely to chromium because it has a weaker *trans* influence than

the chelated phosphorus. Although both of these structures have been solved to give bond lengths that fit the data well, the only bond lengths worth noting are the chromium-oxygen bonds in the two different mixtures, which range from 2.374(3) Å for **13a** to 2.470(3) Å for **13b**. As in the case of the $CrPh_3$ complexes, the room temperature ^2H NMR spectra of **13a** and **13b** in dichloromethane display a single peak at approximately 6 ppm. The room temperature peak for **13** is very broad, indicating that exchange is slower for the $CrPh_2X$ complexes than for the $CrPh_3$ complexes **11** and **12**.

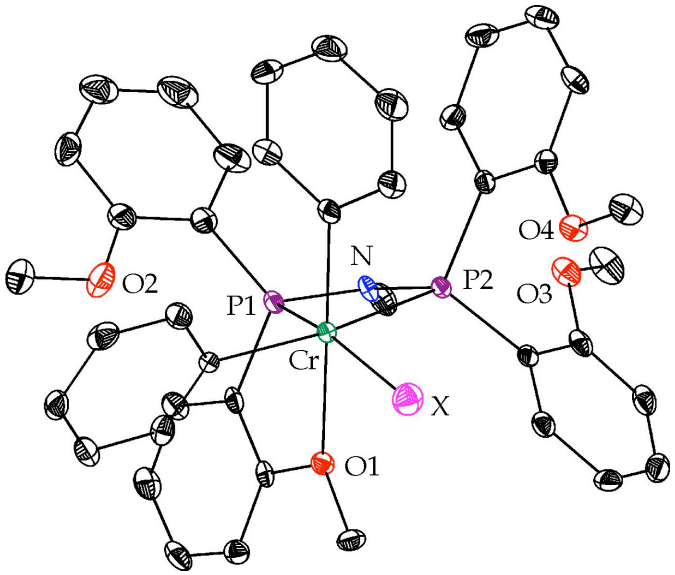

Figure 10. Molecular structure of **13b** with 50% probability ellipsoids.

Synthesis and Characterization of (PNP^{OMe}-d_{12})$CrPh_2Cl$

A variety of attempts have been made to isolate a pure sample of (PNP^{OMe}-d_{12})$CrPh_2Cl$ (**14**). Although dichloromethane is too reactive to allow for isolation of the desired product from the reaction of **11** with Bu_4NCl and $H^+(OEt_2)_2B[C_6H_3(CF_3)_2]_4^-$, the same reaction in chlorobenzene generates the desired product (Scheme 9). However, this route does not provide especially clean product, and the reaction is slow.

Scheme 9.

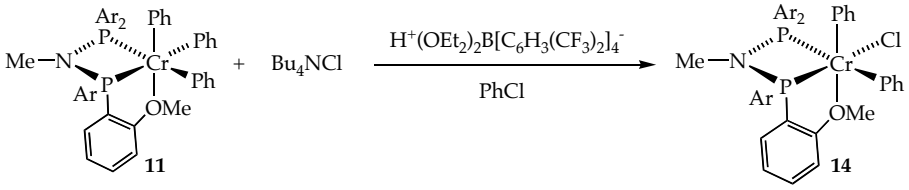

The reaction of $AlCl_3$ with **11** in dichloromethane (Scheme 10) provides a blue-green solid. Slow diffusion of petroleum ether into a dichloromethane solution of the reaction mixture at –35 °C allows for isolation of X-ray quality crystals of this material. The solid state structure of this complex reveals that it is a dimer, with formula $[(PNP^{OMe}\text{-}d_{12})CrPhCl]_2^{2+}/2\ AlCl_4^-$ (**15**), as shown in Figure 11. This complex displays (P,P,O)-κ^3 coordination to chromium, the phenyl groups on chromium are oriented *trans* with respect to one another, and there are two chlorides bridging the chromium atoms. The chromium-oxygen bond lengths are 2.338(4) Å and 2.348(4) Å. As observed for other complexes, this dimer displays shorter bond lengths between chromium and the chelated phosphorus atoms than for the other phosphorus atoms. The chromium-phosphorus bond lengths are 2.412(2) Å and 2.406(2) Å for the chelated phosphorus atoms and 2.510(2) Å and 2.528(2) Å for the other phosphorus atoms. The chromium-chloride bond lengths are 2.3784(19) Å and 2.390(2) Å for one chromium and 2.3709(19) Å and 2.382(2) Å for the other chromium. The chromium-carbon bond lengths are 1.998(6) Å and 2.027(6) Å.

Scheme 10.

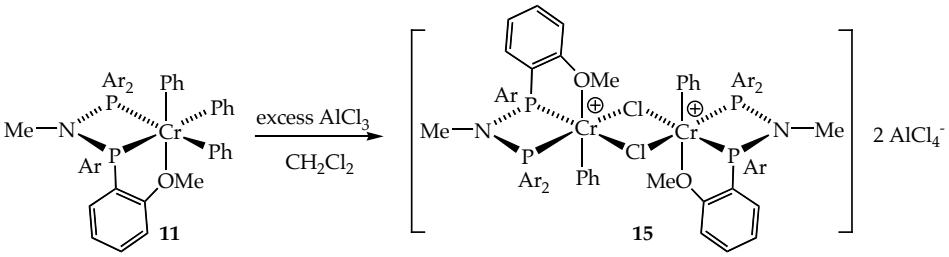

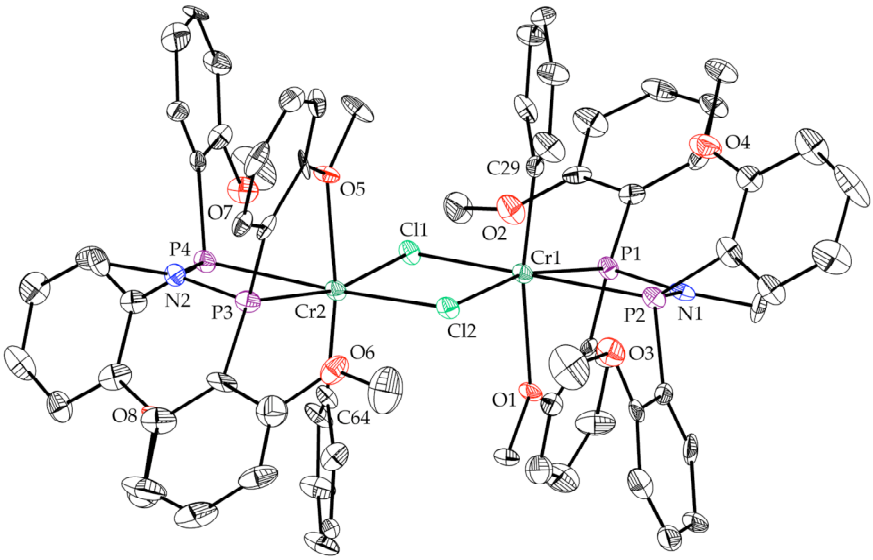

Figure 11. Molecular structure of **15** with 50% probability ellipsoids. The $AlCl_4^-$ anions have been omitted for clarity.

The room temperature ^2H NMR spectrum of the isolated blue-green solid in dichloromethane suggests the presence of multiple products of this reaction. The crystallographically characterized complex **15** may represent only a small percentage of the reaction mixture. The structure of a similar complex, $[(PNP^{OMe})_2Cr_2Me_2Cl_3]^+ / AlCl_4^-$ (**16**), which was isolated by Sara Klamo from the reaction of $CrMeCl_2(THF)_3$ with PNP^{OMe} and $AlMe_3$ in toluene, is shown in Figure 12.[23] This complex is interesting in light of the fact that in the original preparation of the catalyst mixture, $AlMe_3$ and other aluminum species are present from the MAO. These isolated complexes may represent a decomposition pathway for the active catalyst by forming chloride-bridged dimers.

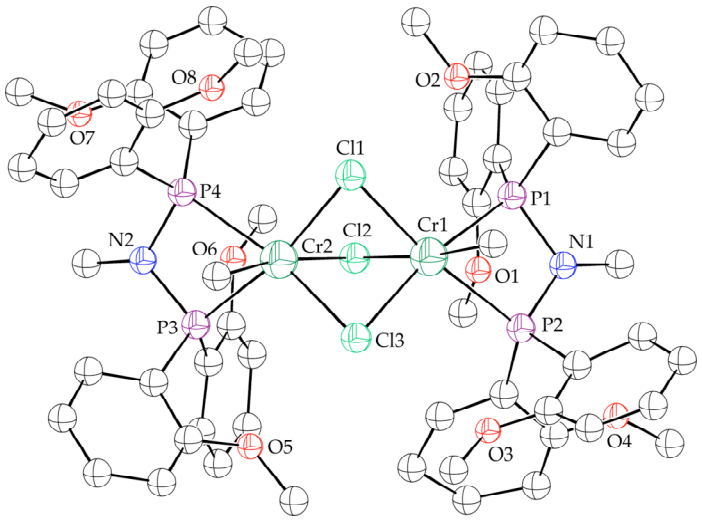

Figure 12. Molecular structure of **16**, with the $AlCl_4^-$ anion omitted for clarity. All atoms were refined isotropically.

The conproportionation reaction between one equivalent of (PNP^{OMe}-d_{12})$CrCl_3$ (**17**), which was originally synthesized by Theodor Agapie as we reported previously,[24] and 2 equivalents of **11** in dichloromethane provides (PNP^{OMe}-d_{12})$CrPh_2Cl$ (**14**) as a dark olive-green powder in 71% isolated yield (Scheme 11). Slow diffusion of petroleum ether into a chlorobenzene solution of **14** at –35 °C provides X-ray quality crystals of this complex. The solid state structure of **14** is shown in Figure 13. This complex is hexacoordinate around chromium and displays (P,P,O)-κ^3 coordination of the PNP^{OMe} ligand with the chloride *trans* to the chelated phosphorus. The chromium-oxygen bond length is 2.4371(14) Å, the chromium-phosphorus bond length for the chelated phosphorus is 2.4414(6) Å, and the other chromium-phosphorus bond length is 2.6096(6) Å. The chromium-chloride bond length is 2.3078(6) Å, which is similar to the chromium-chloride bond length of 2.3210(7) Å observed for the chloride *trans* to the chelated phosphorus in **17**.[24]

Scheme 11.

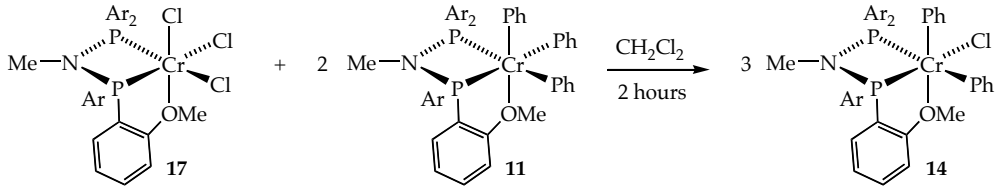

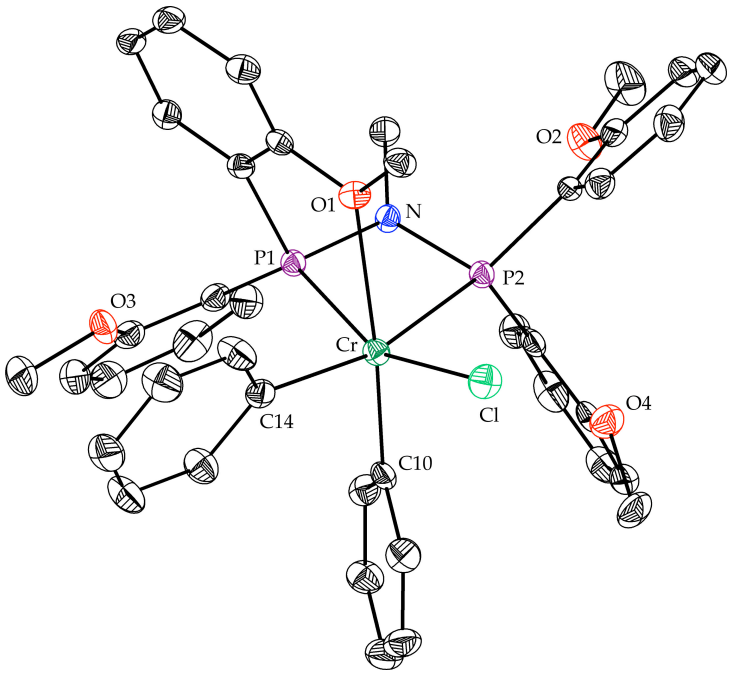

Figure 13. Molecular structure of **14** with 50% probability ellipsoids.

Although the solid state structure of **14** displays the coordination of a single methoxy group to chromium, the room temperature ^{2}H NMR spectrum of **14** in dichloromethane shows a single, very broad peak at δ = 6 ppm (Figure 14). This indicates that an exchange process is occurring to render all four of the methoxy groups equivalent on the ^{2}H NMR time scale. Cooling a dichloromethane solution of **14** displays two distinct coalescence points, both of which are between 0 and 25 °C. These higher temperature coalescence points indicate that the barriers for exchange processes for **14** are higher than for **11**.

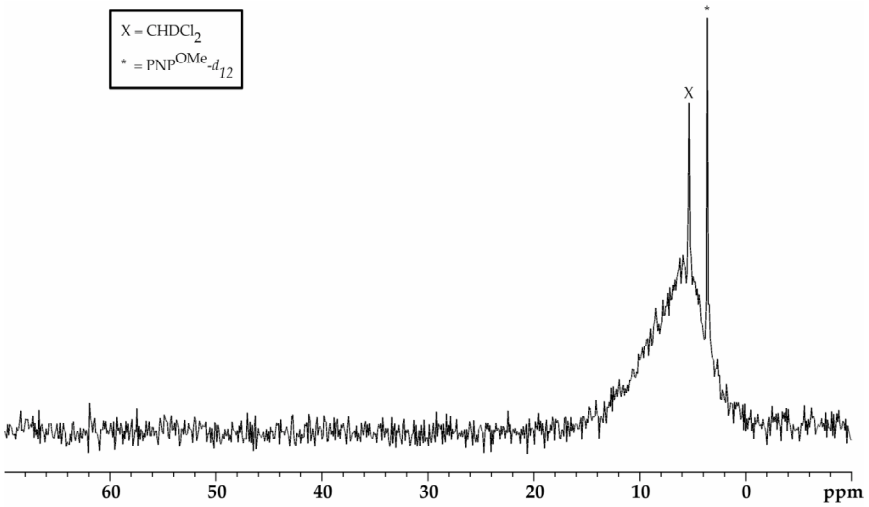

Figure 14. Room temperature ^{2}H NMR spectrum of **14** in dichloromethane.

Unlike in the case of the (PNP)$CrPh_3$ complexes **11** and **12**, the proposed exchange processes involving dissociation and recoordination of methoxy groups for **14** generate different isomers of different energies. The three different isomers and the proposed mechanism for their interconversion are shown in Figure 15. Based on the crystal structure, we assume that the lowest energy isomer is the one in which the chloride is *trans* to the chelated phosphorus. This species can undergo dissociation of a methoxy group followed by recoordination of a methoxy group on the other side of the molecule to generate the isomer in which the chloride is *trans* to the other phosphorus, which is a slightly higher energy isomer. This process occurs on the same hemisphere of the molecule. The resulting isomer can dissociate a methoxy group, undergo a Berry pseudorotation, and recoordinate a methoxy group on the other hemisphere of the molecule to generate the highest energy isomer in which the chloride is *trans* to the coordinated methoxy group and both phenyl groups are *trans* to phosphorus atoms. It is reasonable to suggest that the barriers for exchange processes in **14** are raised as compared to the barriers observed for exchange for the (PNP)$CrPh_3$ complexes as a result of the fact that some of these isomers are higher in energy than others. It is possible that the ground state for **14** is stabilized relative to the ground states for **11** and **12**.

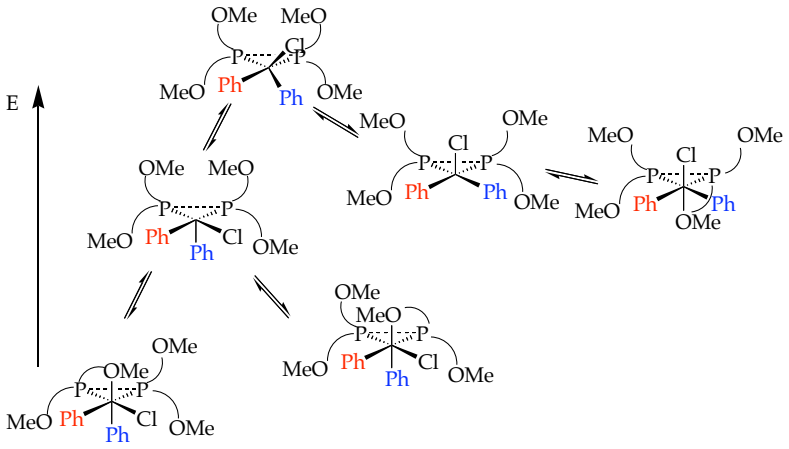

Figure 15. Proposed exchange mechanism for methoxy groups to form different isomers of **14**.

Preparation of (PNP-d_{12})CrPhCl$_2$

It is possible to observe the intermediate formation of (PNP^{OMe}-d_{12})CrPhCl$_2$ (**18**) in the reaction of **17** and **11**. Additionally, **14** undergoes halogenation in dichloromethane solution to form **18**, presumably via a mechanism similar to the radical mechanism that is proposed for the halogenation of **11** (Scheme 8). Therefore, it is critical that the conditions for the conproportionation reaction to make **14** from **11** and **17**, specifically the concentrations of reagents and the duration, are controlled carefully in order to obtain maximum yield and purity of this complex. It can be very difficult to separate **14** from **18**.

Complex **18** may be independently prepared by a conproportionation reaction between 2 equivalents of **17** and one equivalent of **11** in dichloromethane, and it displays two separate ^{2}H NMR signals at room temperature at δ = 4.4 ppm and δ = 11.8 ppm in a 1:1 ratio. The downfield peak is assigned to the two methoxy groups that are exchanging for coordination to chromium, while the upfield peak is assigned to the two methoxy groups that exchange but are never coordinated to chromium. A coalescence process is observed at –65 °C; below this temperature the

complex remains in a static structure with one methoxy group coordinated to chromium, and no exchange processes occur.

As for **14**, there are three different energy isomers of **18** that interconvert in solution. We propose that in the static structure the two chlorides are coordinated to chromium *trans* to the two phosphorus atoms, and the phenyl group is *trans* to the oxygen. Thus, at higher temperatures, exchange of ligands on one hemisphere of the chromium complex, for the coordination site *trans* to the phenyl group, should be facile due to the strong *trans* influence of the phenyl group. Alternatively, Berry pseudorotation to form the isomer of **18** in which a chloride is *trans* to oxygen, a much less stable isomer, has a much higher barrier. As a result, at room temperature, this complex is unable to undergo this type of rotation. There are two isomers of similar high energy in which chloride is *trans* to oxygen. The structure with the chelated phosphorus *trans* to phenyl is of higher energy due to the greater *trans* influence of the more closely bound phosphorus. These exchange processes are illustrated in Figure 16.

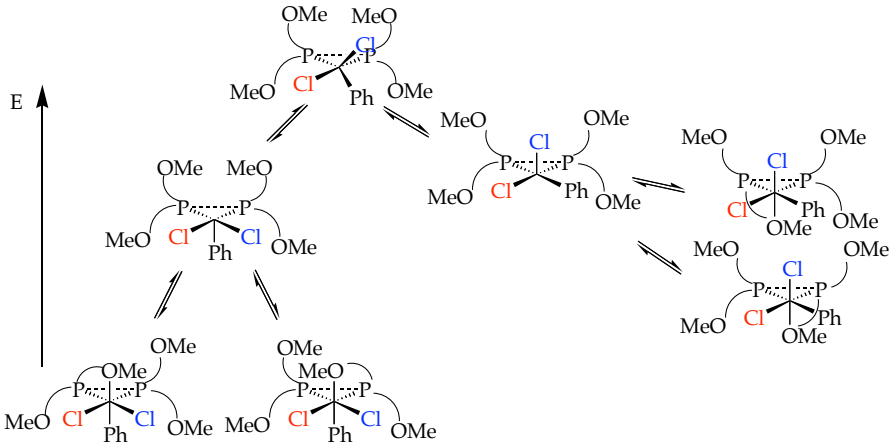

Figure 16. Proposed exchange processes to explain the observation of two distinct coalescence points for **18**.

Structural Comparisons for 11-15, 17, and 18

Comparison of bond lengths and angles from X-ray crystal structures obtained for chromium complexes **11**, **13**, **14**, **15**, and **17**[24] are useful to gain an understanding of the features of PNP ligand **9**. In all cases we observe that the chelated phosphorus is closer to chromium than the other phosphorus by 0.10 – 0.19 Å. We have observed a range of different chromium-oxygen bond lengths for this series of complexes, indicating that the strength of this bond varies significantly with the electronic environment around chromium. A comparison between selected bond lengths and angles for chromium complexes **11**, **13**, **14**, **15**, and **17** is shown in Table 2.

Selected Bond Length (Å) or Angle (°)	**11**[a]	**13a/13b**	**14**	**15**[b]	**17**
Cr-P_1[c]	2.4971	-	2.4414(6)	2.409	2.3855(7)
Cr-P_2	2.6381	-	2.6096(6)	2.519	2.5098(7)
Cr-O	2.286	2.374/2.470	2.4371(14)	2.343	2.1562(15)
Cr-Cl	-	-	2.3078(6)	2.380	2.3210(7)[d]
P-N-P	105.72	-	106.35(9)	107.5	104.95(10)

Table 2. Comparisons between selected bond lengths and angles for complexes **11**, **13**, **14**, **15**, and **17**. [a]Average bond lengths and angles for the two molecules in the unit cell. [b]Average bond lengths and angles for the two molecules in the dimer. [c]P_1 is the chelated phosphorus. [d]The chloride *trans* to the chelated phosphorus.

Comparison of coalescence temperatures associated with exchange processes for coordination of methoxy or thioether groups to chromium in our series of complexes lends insight into the relative lability of these bonds. These coalescence temperatures are shown in Table 3, and we assume that the observation of higher temperature coalescence points correlates with slower rates for the exchange processes. We can thus compare rates for the lower temperature processes, and they may be ordered as **12** > **11** > **18** > **17**[22] > **14**. For the higher temperature process we can order the exchange rates as **11** > **17**[22] > **12** > **14** > **18**. In general we observe that exchange processes occur more

rapidly when all of the X-type ligands on chromium are the same (i.e., all phenyl groups or all chlorides). We believe that the labile coordination of the methoxy or thioether group to chromium that we observe both in the solid state structures of these complexes and by their solution behavior is critical to the unprecedented activity and selectivity for ethylene trimerization observed for this class of catalysts. However, we have yet to determine the optimal binding of these groups to chromium to produce the best catalyst.

Complex	First Coalescence Temperature (°C)	Second Coalescence Temperature (°C)
11	-75	-41
12	-85	5
14	ND[a]	ND[a]
17	-40	-10
18	-65	>25

Table 3. Comparisons between coalescence temperatures for complexes **11**, **12**, **14**, **17**, and **18**. [a]Between 0 and 25 °C.

Reactivity of (PNP)CrPh$_3$ and (PNP)CrPh$_2$Cl Complexes

Both **11** and **14** decompose in toluene solution by reductive elimination of biphenyl. The production of biphenyl by **11** and **14** in toluene solution at room temperature over time has been monitored by GC, and a plot of this data is shown in Figure 17. Complex **11** reductively eliminates biphenyl more quickly than **14**. Presumably once these complexes lose biphenyl, the PNP^{OMe} ligand dissociates from chromium to give an unidentified chromium product. These complexes also decompose in the solid state to give free ligand, which can be observed by ^{2}H NMR spectroscopy, and unidentified chromium products. Again, **11** decomposes more rapidly than **14**.

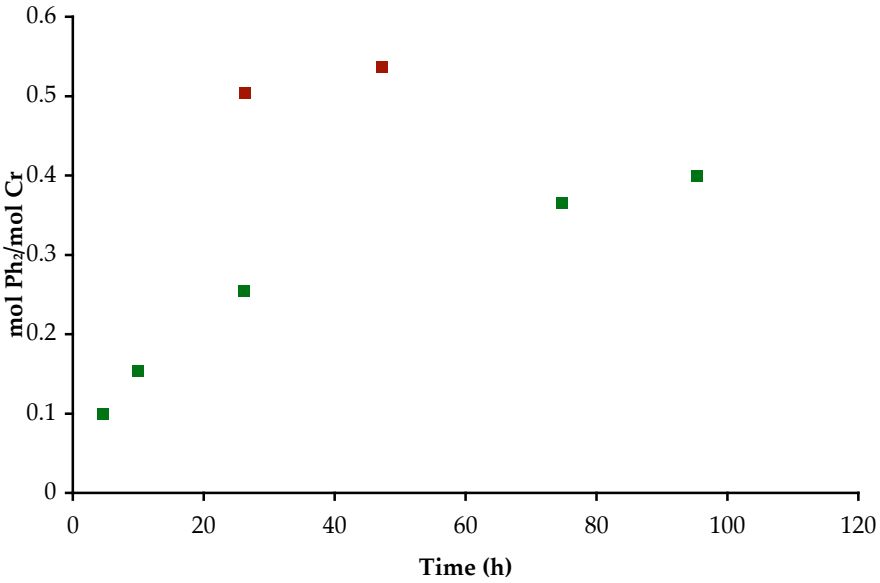

Figure 17. Plot of biphenyl loss by **11** (red) and **14** (green) in toluene solution over time.

Protonation of **11** and halide abstraction from **14** in toluene have been examined. Reactions of **11** with $H^+(OEt_2)_2B[C_6H_3(CF_3)_2]_4^-$ or **14** with $Na^+B[C_6H_3(CF_3)_2]_4^-$ in toluene at room temperature result in rapid formation of green solutions with oily precipitate. Presumably these reactions occur via protonation to give an equivalent of benzene or via halide abstraction to form NaCl, respectively. Benzene is observed in the quenched products of the reaction of **11**; however, to date we have not distinguished the benzene formed by the protonation reaction from benzene formed upon quenching of unreacted chromium-phenyl bonds. We believe that the product of these reactions is $[(PNP^{OMe}\text{-}d_{12})CrPh_2]^+B[C_6H_3(CF_3)_2]_4^-$, in which two methoxy groups may be coordinated to the cationic chromium center, but we do not know the structure of this intermediate. After activation, formation of biphenyl by these systems proceeds very slowly (Scheme 12). In fact, after 22 hours less than 0.5 equivalents of biphenyl are observed.

Scheme 12.

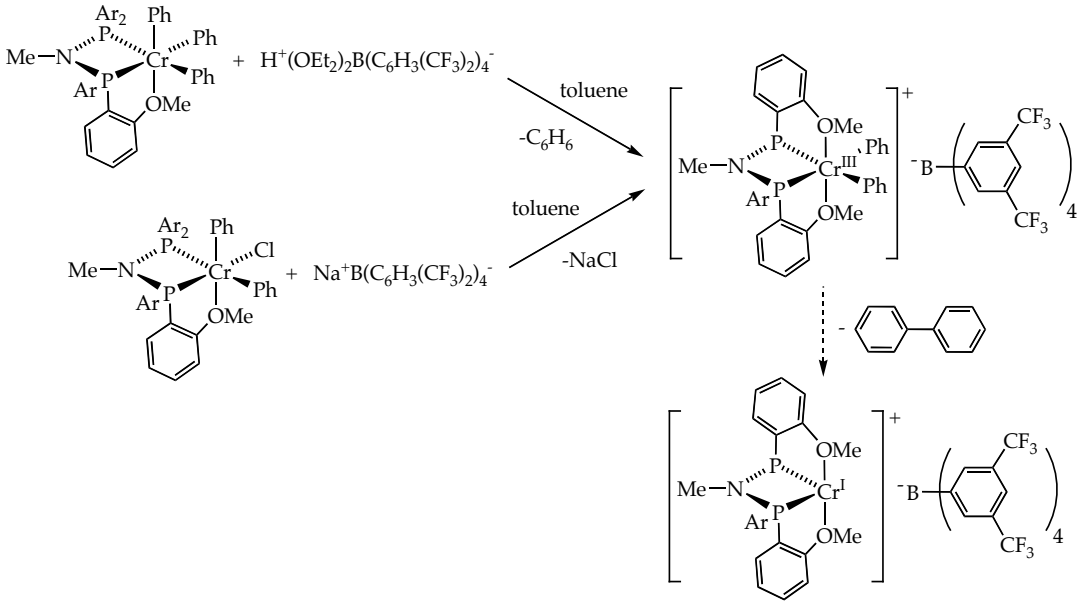

EPR spectra of the reaction of **11** with $H^+(OEt_2)_2B[C_6H_3(CF_3)_2]_4^-$ in the presence of diethyl ether display an 8-line pattern. Protonations of **11** with $H^+(OEt_2)_2B[C_6H_3(CF_3)_2]_4^-$ in either neat diethyl ether or in the presence of diethyl ether in dichloromethane generate a green solution that turns blue over the course of ten hours. The reaction in dichloromethane gives an EPR signal at 15 K, as shown in Figure 18. This species does not give an EPR signal at room temperature, which may be due to zero-field splitting effects.[25] The observed 8-line pattern may be indicative of the presence of a Cr(I) species.[25] However, we do not know whether this is the major species in the reaction mixture. It is possible that the presence of diethyl ether promotes reductive elimination of biphenyl from $[(PNP^{OMe}\text{-}d_{12})CrPh_2]^+$ by stabilizing the resulting Cr(I) species. The phenyl-containing products of this reaction have not been determined.

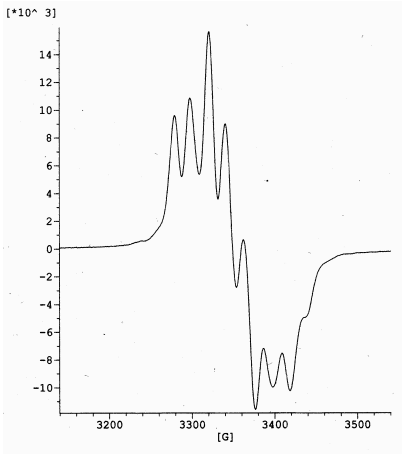

Figure 18. EPR spectrum of **11** and $H^+(OEt_2)_2B[C_6H_3(CF_3)_2]_4^-$ in diethyl ether and dichloromethane at 15 K.

Both **11** and **14** react with ethylene in toluene solution at room temperature to insert ethylene into their chromium-phenyl bonds and form a variety of products over the course of hours. However, formation of 1-hexene is not observed under these conditions. The organic products have been identified by GC and GC-MS after these reactions are quenched; we have not directly observed the chromium complexes that are intermediates or products in these transformations. Insertion of ethylene into chromium-phenyl bonds occurs and is eventually followed by β-hydrogen elimination and reductive elimination to give products with unsaturated and saturated end groups. We observe styrene, ethylbenzene, 4-phenyl-1-butene, and higher ethylene insertion products, as well as benzene. These reactions are shown in Scheme 13.

Scheme 13.

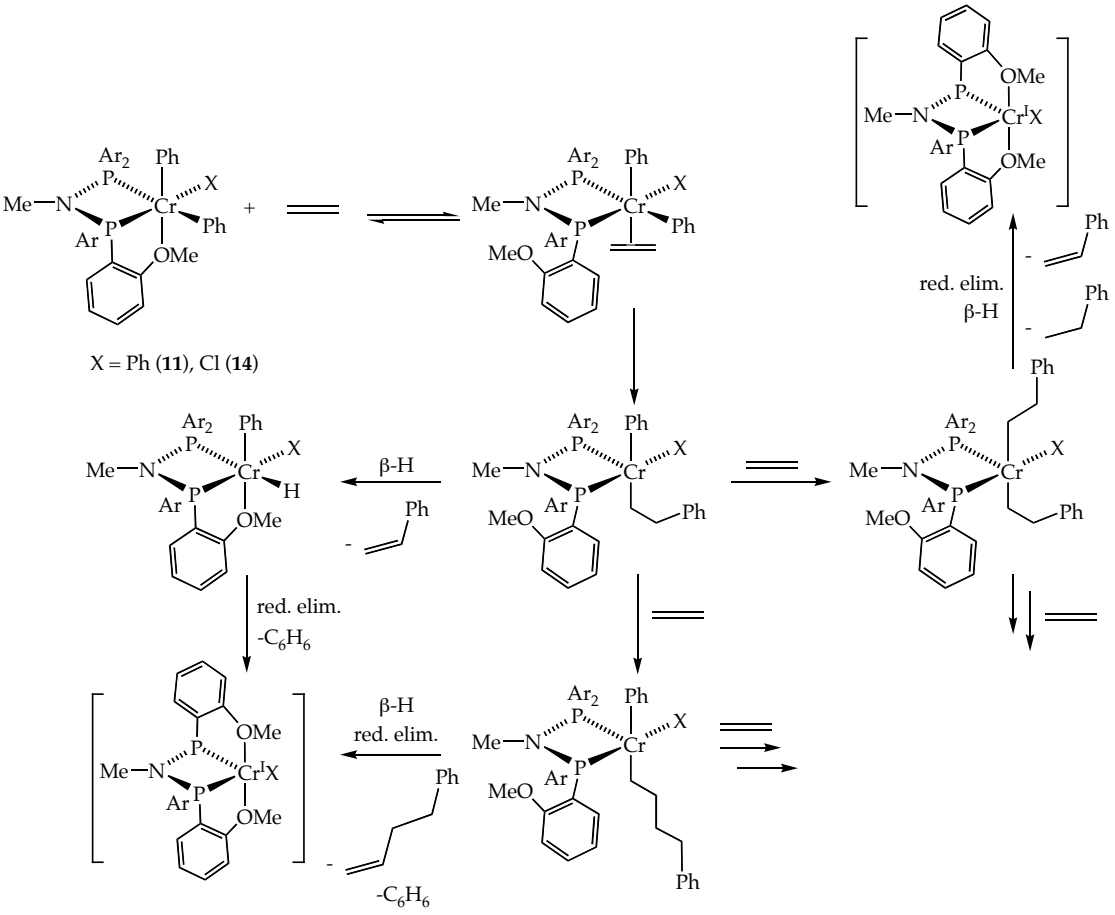

Trimerizations with (PNP)CrPh$_3$ and (PNP)CrPh$_2$Cl Precursors

Once complexes **11** and **14** were made, their activation in the presence of ethylene was examined in order to determine their activity for the trimerization of ethylene. Protonation of **11** with $H^+(OEt_2)_2B[C_6H_3(CF_3)_2]_4^-$ in toluene or abstraction of chloride from **14** with $Na^+B[C_6H_3(CF_3)_2]_4^-$ in chlorobenzene, followed by exposure of the resulting mixture to an atmosphere of ethylene, yield active catalysts for the trimerization of ethylene to 1-hexene (Schemes 14 and 15). These catalysts represent the first examples of well-defined, homogeneous chromium catalysts for the trimerization of ethylene since the discovery of this class of catalysts in 1989.[3] Activation of complexes **11** and **14** provide catalysts that display selectivity similar to the reported bp system. Although catalysis is not always reproducible for these

systems, in part due to their high sensitivity to air and water, under certain conditions these catalysts give turnover numbers to 1-hexene that are on the same order of magnitude as the originally reported bp system.

Scheme 14.

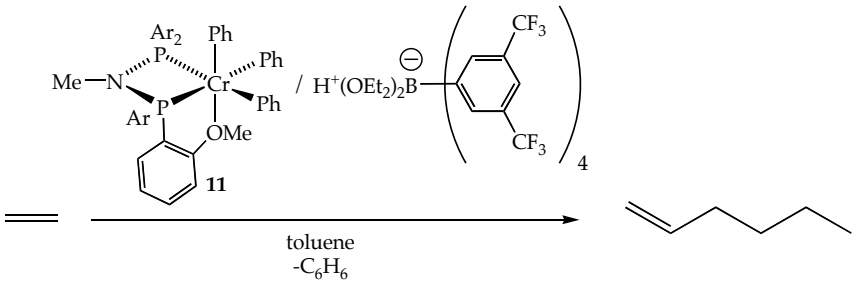

Scheme 15.

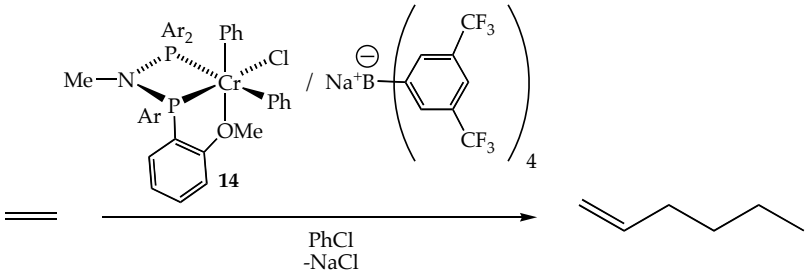

The difference in reactivity with ethylene observed for these activated, presumably cationic species with a non-coordinating anion *versus* the neutral species described above suggests that a cationic species is necessary for catalytic activity. These results also suggest that a non-coordinating anion is necessary for catalyst activity.

In all catalytic runs with **11**/$H^+(OEt_2)_2B[C_6H_3(CF_3)_2]_4^-$ and **14**/$Na^+B[C_6H_3(CF_3)_2]_4^-$ the amounts and concentrations of catalyst used are identical to the conditions reported by bp.[9] These conditions involve exposure of 0.02 mmol of catalyst in 50 mL of toluene to one atmosphere of ethylene at room temperature. We have also examined catalysis in a diethyl ether/toluene solvent mixture, as well as in chlorobenzene. Most of the bp runs lasted 60 minutes; we have varied the times for our runs. Under these

conditions bp reports a turnover number of 4,993 mol 1-hexene/mol chromium. Trimerizations have been carried out on a high vacuum line where ethylene consumption can be monitored with a mercury manometer, and production of 1-hexene has been determined by GC analysis of the organic fractions of quenched reaction mixtures. bp reports that their active catalyst solution is pale green, and we observe that our catalyst mixtures generated from **11**/$H^+(OEt_2)_2B[C_6H_3(CF_3)_2]_4^-$ and **14**/$Na^+B[C_6H_3(CF_3)_2]_4^-$ are a pale green color.

*Trimerizations with **11** and **12***

Although activation of **11** with $H^+(OEt_2)_2B[C_6H_3(CF_3)_2]_4^-$ in toluene generates an active catalyst that produces 1-hexene, catalyst activity is quite variable. In fact, under many conditions turnover numbers are very low and the catalyst seems to be decomposing within 20 minutes. Presumably this system is more moisture-sensitive than the original bp system because it does not have excess MAO present to act as a water scavenger. Figure 19 shows the ethylene consumption over time for two trimerization runs. Under these conditions, turnover numbers less than 10 mol 1-hexene/mol chromium are observed after a 60 minute run.

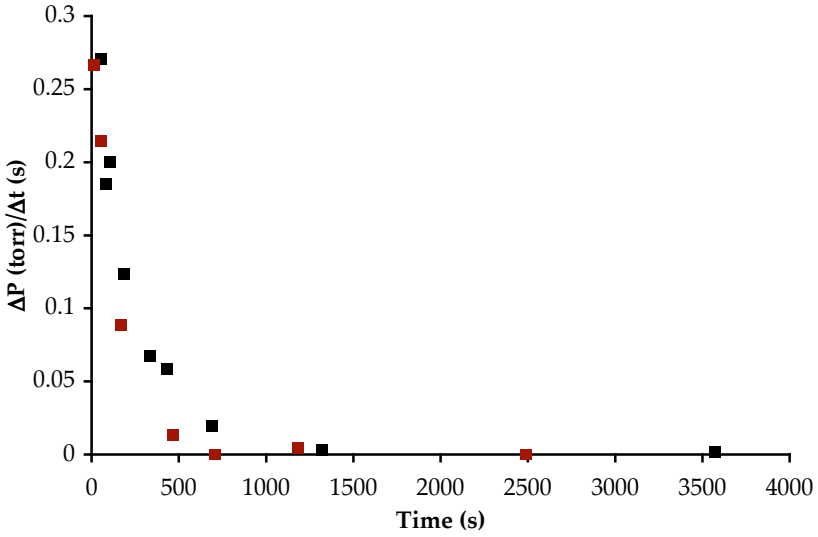

Figure 19. Ethylene consumption over time for two trimerizations catalyzed by **11** activated with $H^+(OEt_2)_2B[C_6H_3(CF_3)_2]_4^-$ in toluene.

These data can be analyzed using differential equations to determine that the catalyst decomposition is first-order in chromium. A general rate law for the reaction of chromium with ethylene can be written as shown in Equation 1, which depends on [ethylene]^2 and [Cr], according to the observations of bp.[9] Substitution of k_c, which represents the rate of catalysis in the absence of decomposition, for $-k$[ethylene]^2 gives Equation 2, which can be rearranged to Equation 3. The concentration of chromium ([Cr]) is related to dP/dt, assuming that the concentration of active chromium catalyst is directly proportional to the ethylene consumption over time (A = constant, Equation 4). Equation 5 is an expression for the loss of chromium over time that is first-order in chromium and has a decomposition rate of k_d. Rearranging this equation (Equation 6) and integrating the expression gives Equation 7. Finally, substituting the value of [Cr] from Equation 3 into Equation 7 gives Equation 8. Equation 8 can be rearranged to give Equation 9, from which it is clear that if the plot of ln(dP/dt) *versus* time is linear, then the decomposition of the catalyst is first-order in chromium. Additionally the

slope of this line is the decomposition rate k_d, and the y-intercept of this line is $\ln(k_c)$.

$$\text{rate} = -\frac{\text{dP}}{\text{dt}} = k[\text{ethylene}]^2[\text{Cr}] \quad (1)$$

$$\frac{\text{dP}}{\text{dt}} = k_c[\text{Cr}] \quad (2)$$

$$[\text{Cr}] = \left(\frac{1}{k_c}\right)\left(\frac{\text{dP}}{\text{dt}}\right) \quad (3)$$

$$[\text{Cr}] = \text{A}\left(\frac{\text{dP}}{\text{dt}}\right) \quad (4)$$

$$-\frac{[\text{Cr}]}{\text{dt}} = k_d[\text{Cr}] \quad (5)$$

$$\frac{\text{d}[\text{Cr}]}{[\text{Cr}]} = -k_d\ \text{dt} \quad (6)$$

$$\ln[\text{Cr}] = -k_d\text{t} \quad (7)$$

$$\ln[\text{Cr}] = \ln\left(\frac{\text{dP}}{\text{dt}}\right) - \ln(k_c) = -k_d\text{t} \quad (8)$$

$$\ln\left(\frac{\text{dP}}{\text{dt}}\right) = -k_d\text{t} + \ln(k_c) \quad (9)$$

In fact, a plot of the natural log of ethylene consumption *versus* time gives a straight line, as shown in Figure 20, suggesting that this catalyst decomposition is first-order in chromium. In the case of these trimerizations the rate of decompostion (k_d) is approximately 10^{-3} s^{-1}, and the rate of catalysis (k_c) is 0.27 s^{-1}.

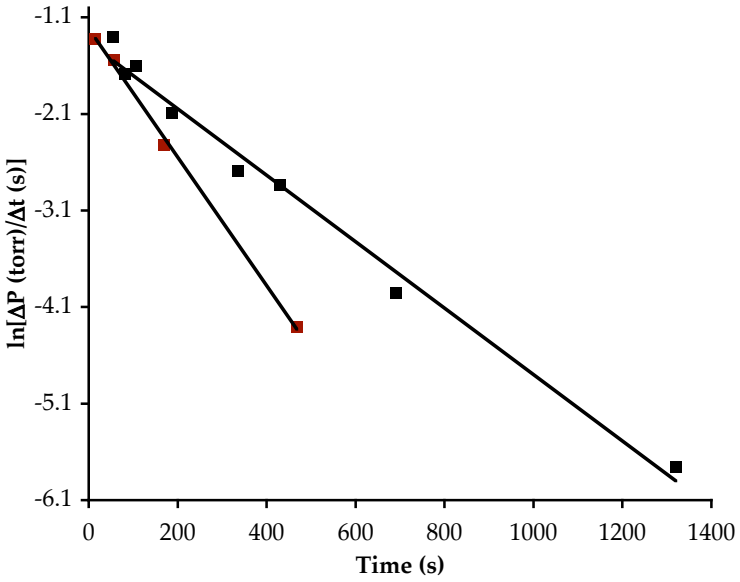

Figure 20. Plot of the natural log of ethylene consumption over time *versus* time for trimerizations catalyzed by **11** activated with $H^+(OEt_2)_2B[C_6H_3(CF_3)_2]_4^-$ in toluene.

Evidence suggests that the presence of an L-type donor may be key to catalytic activity, as it may serve to solubilize or stabilize the active catalyst. We observe that the catalyst often oils out of toluene. Additionally, bp observes lower turnover numbers for the trimerization when they activate an "isolated" catalyst, presumably $(PNP^{OMe})CrCl_3$, as compared to their *in situ* preparation of the catalyst from the $CrCl_3(THF)_3$ precursor.[9b] Finally, we have observed lower turnover numbers for trimerizations run in freshly collected or vacuum transferred solvents that have not been contaminated with THF or diethyl ether that are present in the glove box atmosphere.[26]

Activation of the catalyst in the presence of diethyl ether dramatically increases the lifetime and activity of the catalyst. In fact, in at least one case, protonation of **11** with $H^+(OEt_2)_2B[C_6H_3(CF_3)_2]_4^-$ in diethyl ether (2 mL, approximately 900 equivalents), followed by addition of 48 mL of toluene and exposure to an atmosphere of ethylene yields a catalyst that remains active for at least three hours to give a turnover number of 2,780 mol 1-hexene/mol

chromium in six hours. This turnover number is of the same order of magnitude as for the originally reported bp system. A plot of the ethylene consumption over time for this catalyst is shown in Figure 21.

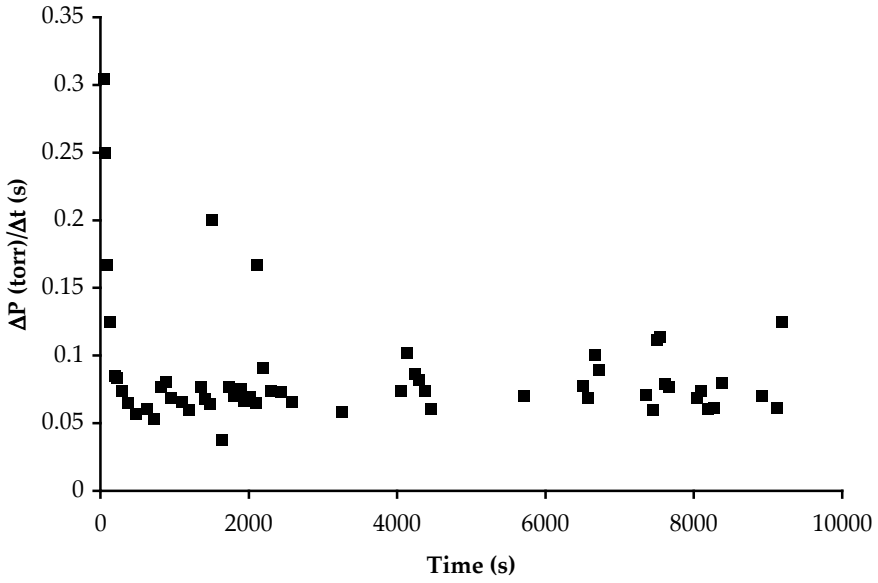

Figure 21. Ethylene consumption over time for trimerization catalyzed by **11** activated with $H^+(OEt_2)_2B[C_6H_3(CF_3)_2]_4^-$ in diethyl ether and toluene.

However, despite this encouraging result, we have been unable to reproduce this exact procedure to generate a living catalyst. In some cases, this same procedure generates a totally inactive catalyst. In other cases, catalysts are formed that have some activity but decompose quickly and give low turnover to 1-hexene. While this procedure often generates an active catalyst, the species still oils out of solution over time. The ethylene consumption over time is shown in Figure 22 for another example of an attempt of the identical catalyst preparation. In this case the catalyst takes almost 20 minutes to initiate, its activity increases, and then it begins to deactivate in less than three hours, to give a final turnover number of 1,793 mol 1-hexene/mol chromium for a three hour run. Attempts to run trimerizations in 50 mL of diethyl ether solvent in the absence of toluene generate species that do not consume ethylene.

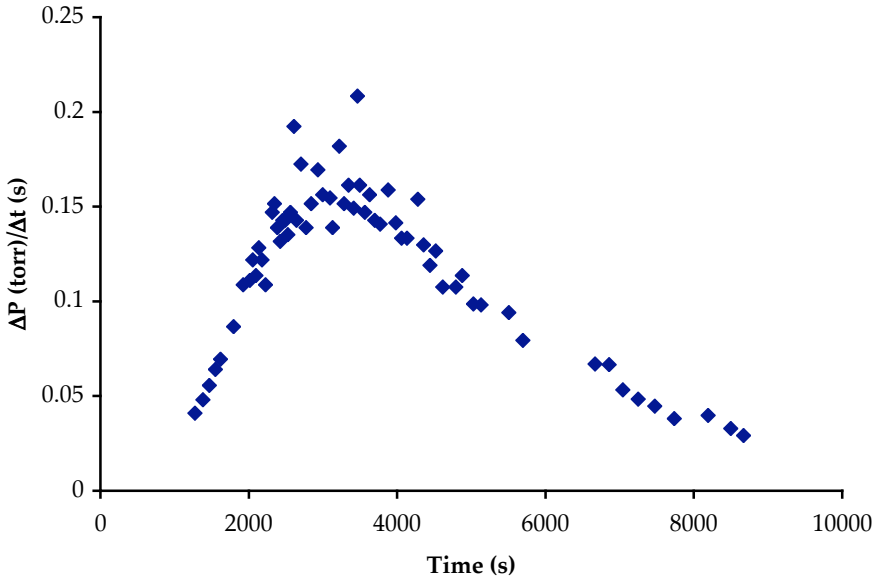

Figure 22. Ethylene consumption over time for trimerization catalyzed by **11** activated with $H^+(OEt_2)_2B[C_6H_3(CF_3)_2]_4^-$ in diethyl ether and toluene.

Complex **11** can also be activated by $H^+(OEt_2)_2B[C_6H_3(CF_3)_2]_4^-$ in the presence of 900 equivalents of diethyl ether in 48 mL of chlorobenzene to provide an active catalyst. Plots of ethylene consumption over time for two trimerizations using these conditions are shown in Figure 23. Neither of these catalysts undergoes an initiation period; however, they both decompose over the course of one hour, and they both give turnover numbers of approximately 735 mol 1-hexene/mol chromium. Following the analysis presented above, we find that the catalysts formed under these conditions decompose via a first-order process with a decomposition rate of approximately 10^{-4} s^{-1} and a rate of catalysis (k_c) of approximately 5 X 10^{-2} s^{-1}. Unlike in toluene, the catalyst does not oil out of chlorobenzene solution. However, chlorobenzene may react with a $[(PNP^{OMe})Cr^{I}]^+$ species via oxidative addition to make $[(PNP^{OMe})Cr^{III}PhCl]^+$, which may explain the more rapid decomposition of the active catalyst under these conditions.

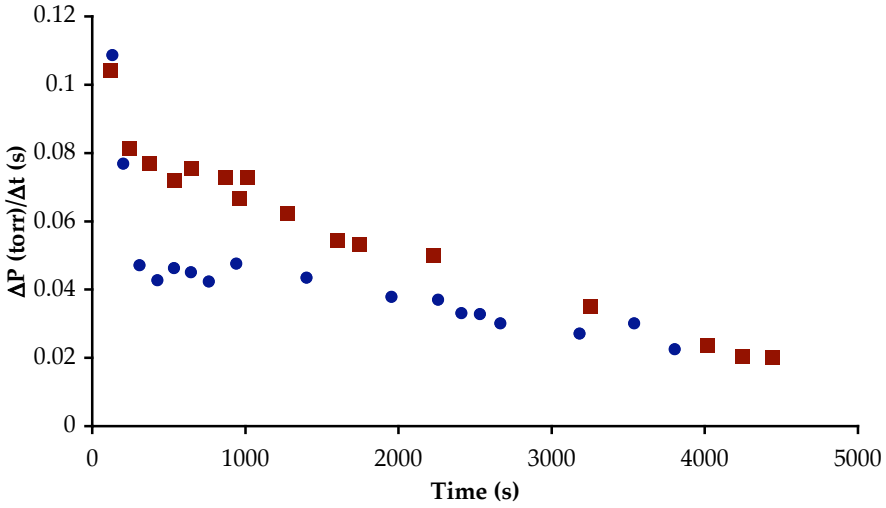

Figure 23. Ethylene consumption over time for trimerizations catalyzed by **11** activated with $H^+(OEt_2)_2B[C_6H_3(CF_3)_2]_4^-$ with diethyl ether in chlorobenzene.

It is possible to activate **11** with $Me_2PhNH^+B[C_6F_5]_4^-$ to generate an active catalyst. Addition of 900 equivalents of diethyl ether to **11** and $Me_2PhNH^+B[C_6F_5]_4^-$, followed by addition of 48 mL of toluene and exposure to one atmosphere of ethylene, generates a catalyst that remains active for almost two hours. Ethylene consumption over time for this catalyst is shown in Figure 24. This catalyst undergoes a rapid initiation period, followed by rapid decomposition, and achieves a final turnover number of 3,046 mol 1-hexene/mol chromium in two hours, which is the highest turnover number we have observed for the $(PNP)CrPh_3$ system to date.

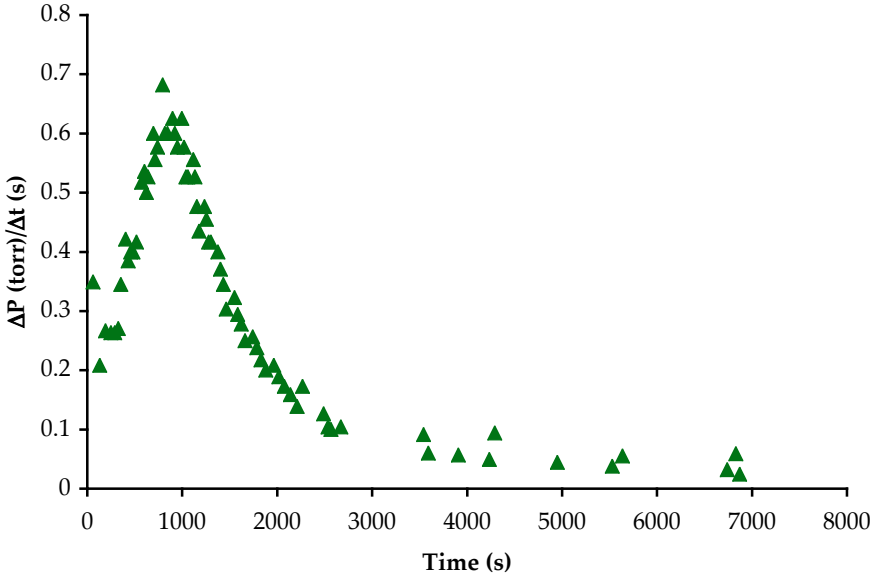

Figure 24. Ethylene consumption over time for trimerization catalyzed by **11** activated with $Me_2PhNH^+B[C_6F_5]_4^-$ with diethyl ether in toluene.

Finally, **11** can be activated with MAO to produce an active catalyst for the trimerization of ethylene. Addition of 300 equivalents of MAO to a toluene solution of **11** under an atmosphere of ethylene causes the solution to turn from red-brown to green-brown and consume ethylene. Ethylene consumption over time for this catalyst is shown in Figure 25. Unlike other catalysts preparations, this species does not seem to have an initiation period, and it does not oil out during the reaction. This catalyst produces 1,494 mol 1-hexene/mol chromium over one hour, but it does undergo first order decomposition with a rate of approximately 10^{-3} s^{-1}.

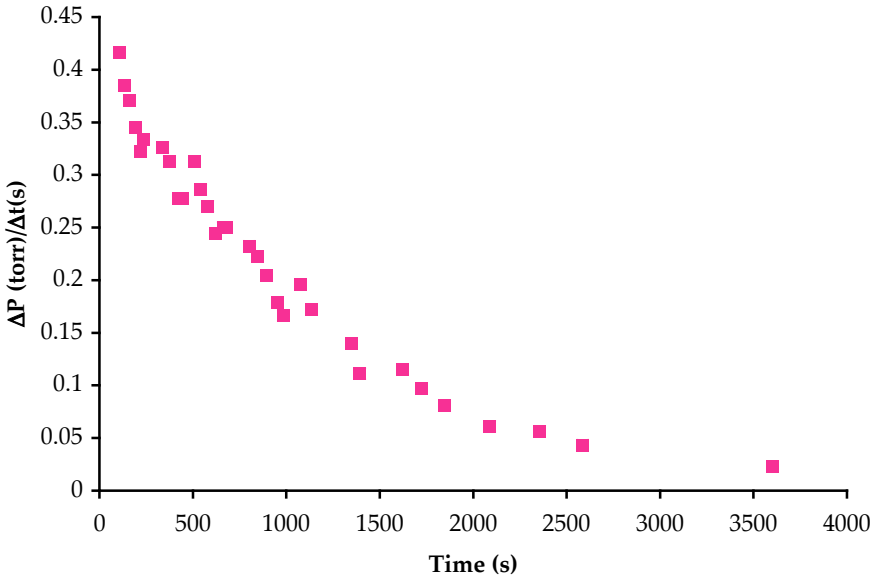

Figure 25. Ethylene consumption over time for **11** activated with MAO in toluene.

Attempts to activate (PNP^{SMe}-d_{12})$CrPh_3$ (**12**) gave no ethylene trimerization activity, even at elevated temperatures. Activation of **12** with MAO in toluene provides a green solution that does not consume ethylene. Attempts to heat this mixture to 95 °C under an atmosphere of ethylene do not create an active trimerization catalyst. However, to date, no attempts have been made to activate **12** by protonation.

*Trimerizations with **14***

Activation of (PNP^{OMe}-d_{12})$CrPh_2Cl$ (**14**) with $Na^+B[C_6H_3(CF_3)_2]_4^-$ in chlorobenzene provides an active catalyst for the trimerization of ethylene. Ethylene consumption for trimerizations run with this catalyst preparation was not monitored; instead production of 1-hexene for runs of different times was determined after reactions were quenched. A plot of moles of 1-hexene produced per mole of chromium over time for three different trimerization runs is shown in Figure 26. This catalyst gives turnovers to 1-hexene of less than 447 mol 1-hexene/mol chromium at all reaction times, which are an

order of magnitude less than those observed with the (PNP)$CrPh_3$ system or by bp. Although 1-hexene production does increase over time, it does not appear to increase linearly, suggesting that this catalyst system also undergoes decomposition. However, conditions for this reaction have not been optimized.

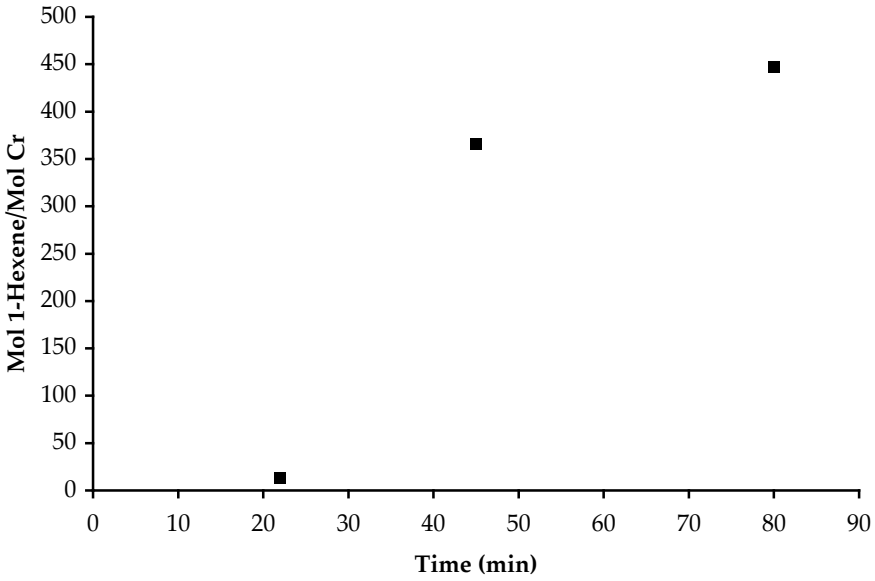

Figure 26. Production of 1-hexene by **14** activated with $Na^+B[C_6H_3(CF_3)_2]_4^-$ in chlorobenzene for trimerizations of different times.

Trimerizations with $CrCl_3(THF)_3$/PNP/MAO

In order to understand some of the factors that affect catalyst activity and lifetime, we have examined trimerizations with the bp system under identical conditions as described above in our laboratory. It is possible that a better understanding of the bp system will lend insight into the cause of our highly variable results with the (PNP)$CrPh_3$ catalyst system and ultimately allow us to prepare a more stable catalyst from our well-defined (PNP)$CrPh_3$ precursor. We find that in all cases our preparation of the bp system leads to an active catalyst for ethylene trimerization. However, the catalysts generated undergo decomposition that appears first-order in chromium with

a rate of approximately 10^{-4} s^{-1}, and they do not give turnover to 1-hexene as high as the originally reported system. Additionally, in almost all cases, these catalysts have an initiation period, during which time their activity increases, and after which time their activity decreases. Overall we observe that this catalyst is very sensitive to small changes in the system; for example, using MAO from a different source gives turnover numbers that are almost an order of magnitude less than those observed by bp.

In fact, a trimerization run using the catalyst preparation identical to the bp conditions gives 1,670 mol 1-hexene/mol chromium over one hour.[9] This preparation of the catalyst, in which the PNP and $CrCl_3(THF)_3$ mixture are activated with MAO solution before exposure to ethylene, provides a species that does not have a significant initiation period. The lack of initiation period may be due in part to the fact that the catalyst mixture is allowed to react for up to ten minutes before exposure to ethylene. This catalyst does decompose over the course of one hour. On the other hand, activation of the mixture of PNP and $CrCl_3(THF)_3$ with MAO solution after the mixture has been exposed to an atmosphere of ethylene provides a catalyst that takes about eight minutes to initiate fully, and it then begins to decompose. This catalyst gives a better turnover number of 2320 mol 1-hexene/mol chromium over one hour. Plots of the ethylene consumption over time for these catalysts are shown in Figure 27.

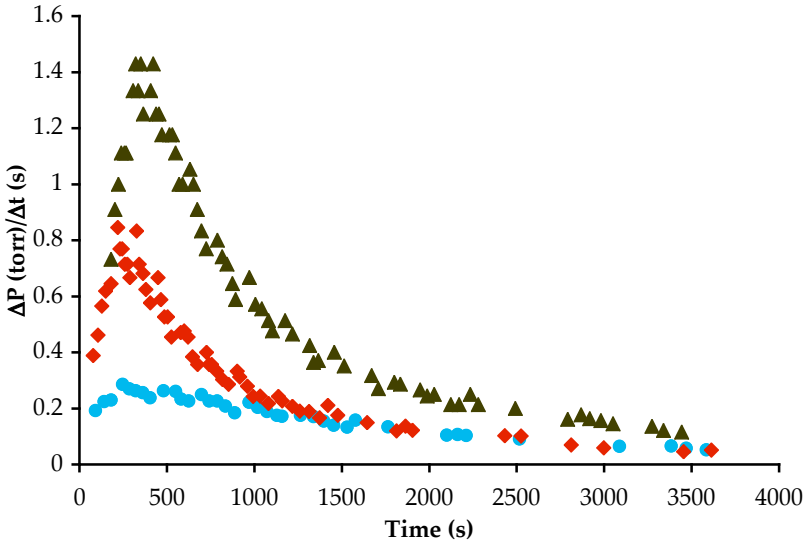

Figure 27. Ethylene consumption over time for catalysts generated from a mixture of PNP^{OMe} and $CrCl_3(THF)_3$ activated by MAO in toluene following the original bp conditions (blue circles); activated by MAO after exposure of the mixture to ethylene (red diamonds); and activated by MAO after exposure to ethylene, using 50% less chromium in the same total volume (brown triangles).

Decreasing the catalyst concentration in solution by 50% doubles its production of 1-hexene. This catalyst gives a turnover number of 4,630 mol 1-hexene/mol chromium in one hour. This turnover number is the highest we have obtained and is the closest number to the originally reported bp numbers that we have observed to date. However, as for all of the other cases, this methodology produces a catalyst that undergoes an initiation period followed by decomposition. A plot of ethylene consumption over time for this catalyst is shown in Figure 27. A plot of the natural log of ethylene consumption over time *versus* time for trimerization catalyzed by PNP^{OMe} and $CrCl_3(THF)_3$ activated by MAO in toluene is shown in Figure 28. This plot allows for determination of the rates of decomposition for these catalysts. In the case of the catalyst that is activated with MAO prior to exposure to ethylene the rate of decomposition is approximately 5×10^{-4} s^{-1},

while for both of the other trials involving MAO addition after exposure to ethylene, the rate of decomposition is approximately 10^{-3} s^{-1}.

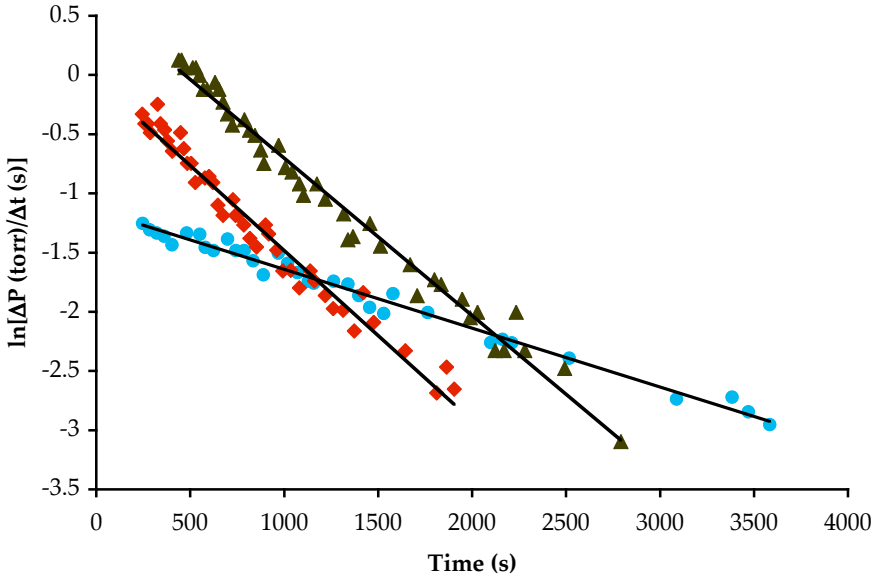

Figure 28. Plot of the natural log of ethylene consumption over time *versus* time for trimerization catalyzed by PNP^{OMe} and $CrCl_3(THF)_3$ activated by MAO in toluene following the original bp conditions (blue circles); activated by MAO after exposure of the mixture to ethylene (red diamonds); and activated by MAO after exposure to ethylene, using 50% less chromium in the same total volume (brown triangles).

Attempts to utilize PNP^{SMe} as a ligand for trimerization under these conditions gave no reaction. A toluene solution of **10** and $CrCl_3(THF)_3$ appears purple, and activation of this mixture with MAO produces a green-brown solution. Exposure of this species to an atmosphere of ethylene does not result in the production of 1-hexene. It is possible that **10** does not bind to the chromium of $CrCl_3(THF)_3$ under these conditions.

Mechanistic Studies on the Ethylene Trimerization System

A mechanism for formation of 1-hexene by chromium catalysts involving metallacyclic intermediates has been favored over a Cossee-type mechanism, in large part because the latter offers no reasonable explanation for highly selective ethylene trimerization.[3] A Cossee-type mechanism, shown in Scheme 16, involves insertions of ethylene into chromium-hydride or chromium-alkyl bonds, as is typically the mechanism for polymerization or oligomerization of olefins, followed by β-hydrogen elimination to give 1-hexene. However, it is difficult to explain why this system would selectively undergo β-hydrogen elimination after insertion of three ethylenes. Aside from the experiment by Jolly and co-workers, in which the chromacycloheptane complexes decompose more readily than chromacyclopentane complexes to yield 1-hexene,[27] no experiment has been reported to distinguish between these alternative mechanisms.

Scheme 16.

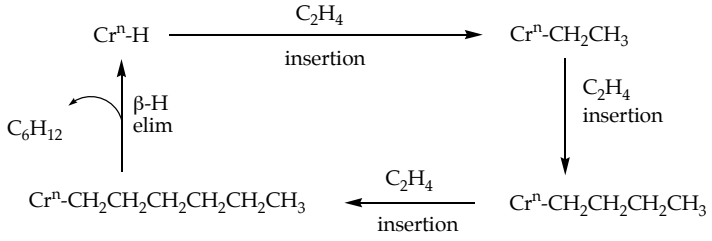

Trimerization of a 1:1 mixture of C_2D_4/C_2H_4 provides an experimental way to probe the mechanism of 1-hexene formation. A route involving metallacyclic intermediates would give no H/D scrambling to produce only C_6D_{12}, $C_6D_8H_4$, $C_6D_4H_8$, and C_6H_{12}, while the Cossee-type mechanism would lead to H/D scrambling and formation of 1-hexene isotopomers containing an odd number of deuterons. In fact, addition of an equimolar mixture of C_2D_4 and C_2H_4 to the catalyst obtained by activating **11** with $H^+(OEt_2)_2B[C_6H_3(CF_3)_2]_4^-$ produces only the isotopomers C_6D_{12}, $C_6D_8H_4$, $C_6D_4H_8$, and C_6H_{12} in an approximately 1:3:3:1 ratio, the statistically expected

ratio for a mechanism involving metallacyclic intermediates. The GC and MS traces of the 1-hexene region for these trimerizations are shown in Figures 29 and 30. A 1:3:3:1 1-hexene isotopomer distribution is obtained for the catalyst prepared from the original bp system, $CrCl_3(THF)_3$/PNP^{OMe}/MAO, as well as other catalyst preparations, indicating that the same type of mechanism is in effect for all of the cases analyzed.[24] This data supports a mechanism involving metallacyclic intermediates, and represents the first experimental support for this mechanism with a working catalyst system.

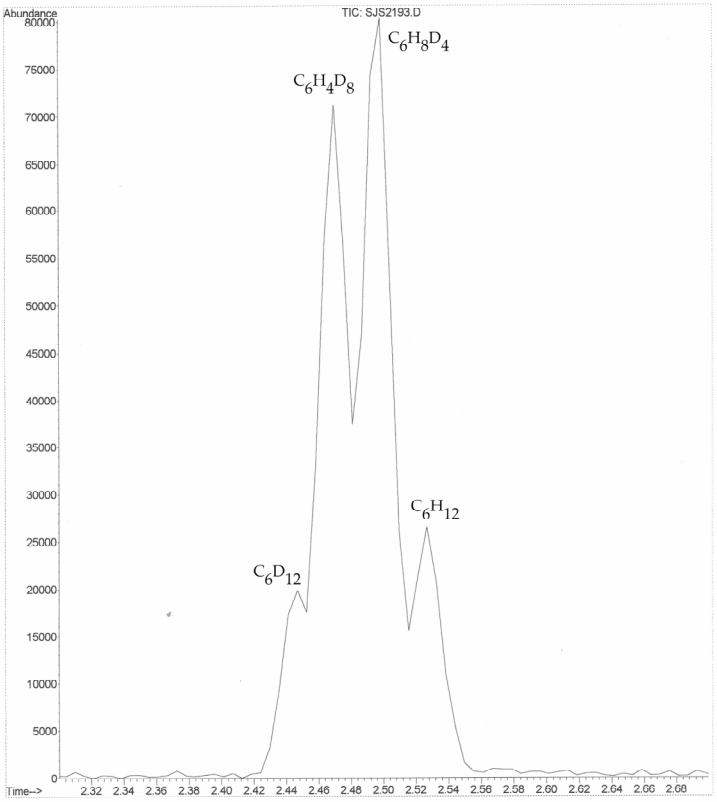

Figure 29. GC trace of the hexene region of a trimerization of a 1:1 mixture of C_2H_4 and C_2D_4 catalyzed by **11** activated with $H^+(OEt_2)_2B[C_6H_3(CF_3)_2]_4^-$.

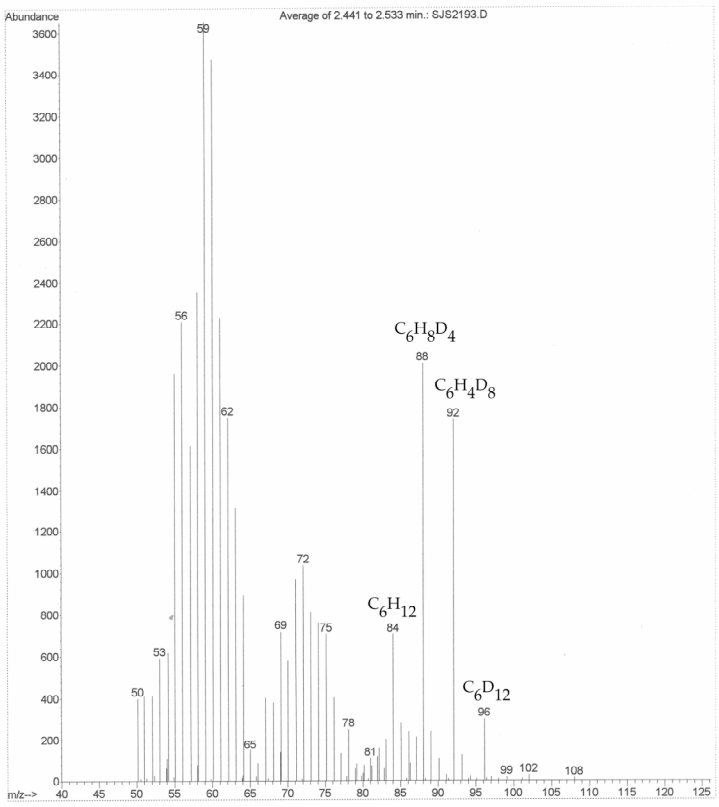

Figure 30. MS trace of the hexene region of a trimerization of a 1:1 mixture of C_2H_4 and C_2D_4 catalyzed by **11** activated with $H^+(OEt_2)_2B[C_6H_3(CF_3)_2]_4^-$.

Initiation Mechanisms for 11 and 14

By analyzing and quantifying the phenyl-containing organic products generated in trimerization reactions catalyzed by **11** or **14**, we have determined the mechanism of initiation for this family of catalysts. We have examined the phenyl-containing products under conditions where **11** or **14** are activated in solution, rapidly exposed to an atmosphere of ethylene, the trimerization reaction is run for a given time, and the reaction mixture is quenched with water. We have already discussed that activations of **11** and **14** proceed rapidly to generate $[(PNP^{OMe}\text{-}d_{12})CrPh_2]^+B[C_6H_3(CF_3)_2]_4^-$ (*vide supra*). Once exposed to ethylene, this species may undergo reductive elimination of biphenyl or insert ethylene into a chromium-phenyl bond. In the absence of ethylene, we know that reductive elimination of biphenyl is slow, and we observe only trace amounts of biphenyl under trimerization conditions. We

do observe formation of styrene and other phenyl-containing products under trimerization conditions.

Thus we conclude that chromium-phenyl bonds are cleaved primarily by ethylene insertion, which is eventually followed by β-hydrogen elimination and reductive elimination to give phenyl-containing products with both unsaturated and saturated end groups. The products are similar to those observed in the reaction of ethylene with the neutral species **11** and **14**. Some possible reaction pathways for the activated species are shown in Scheme 17. More thorough quantification of the various phenyl-containing products will give us insight into the relative rates of these processes. Additionally, characterization of these products when **11** is protonated in the presence of diethyl ether may provide information about the role of this additive in improving trimerization activity.

Scheme 17.

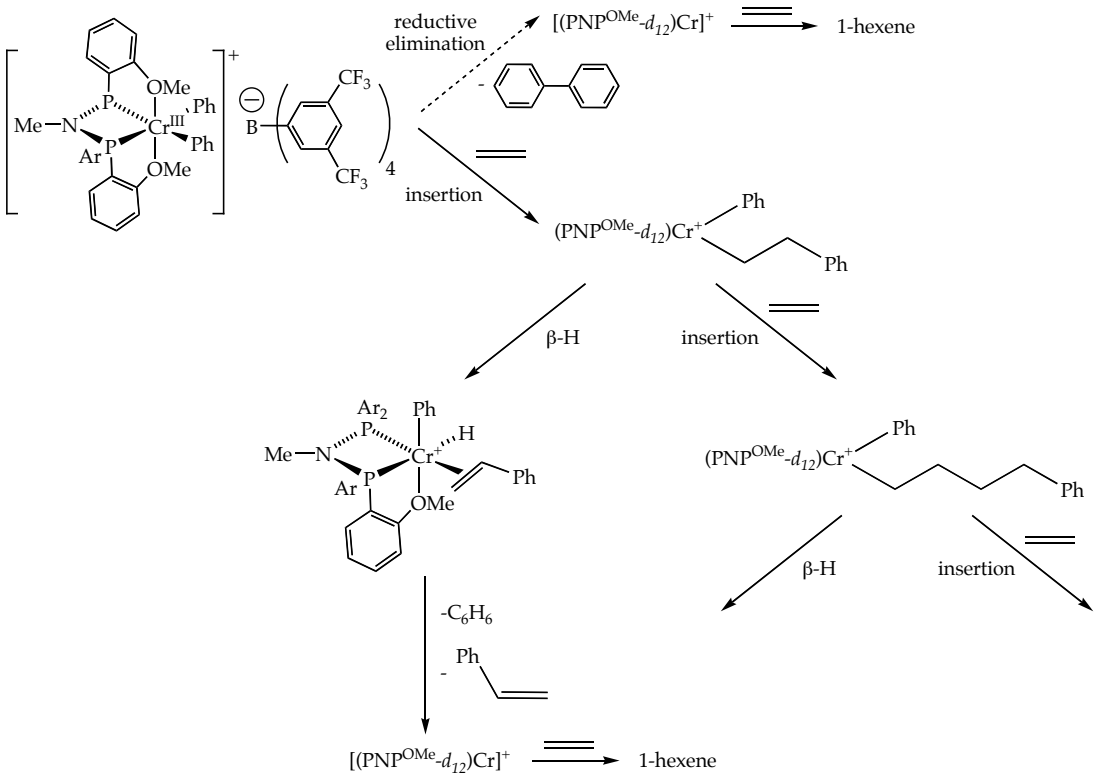

Conclusions

A variety of phenyl chromium(III) complexes containing PNP ligands have been prepared and characterized both in solution and in the solid state. We have examined the chromium triphenyl complexes of two PNP ligands, one containing aryl groups with *ortho*-methoxy groups (PNP^{OMe}) and the other containing *ortho*-methylthioether (PNP^{SMe}) groups. These complexes both display octahedral geometries around chromium in the solid state, but the PNP^{OMe} ligand coordinates with two phosphorus atoms and one oxygen, while the PNP^{SMe} coordinates through two sulfur atoms and one phosphorus. These different binding modes indicate the flexibility of this family of complexes to choose to bind the donor that best matches the steric and electronic environment around chromium. We have examined the solid state structure of the PNP^{OMe} complex of chromium diphenyl chloride, and we observe similar binding as seen for the triphenyl complex of this ligand. Amongst all of the complexes studied by X-ray crystallography, we observe a range of chromium-oxygen bond lengths, indicating that the strength of this bond is especially sensitive to the coordination environment around chromium.

We have also studied the solution behavior of these complexes by variable temperature ^2H NMR spectroscopy and observe that in all cases they undergo dynamic exchange processes at room temperature. We have proposed the two distinct exchange processes to explain the variable temperature behavior observed. We believe that it is this labile coordination of oxygen to chromium that provides a unique catalyst environment. The labile coordination of the methoxy groups may be critical to the high selectivity to 1-hexene, as well as to the unprecedented activities of these complexes.

From the chromium triphenyl and diphenyl chloride complexes of PNP^{OMe}, we have prepared ethylene trimerization catalysts. These catalysts

display selectivity and activity similar to the bp system, and they represent the first example of well-defined chromium-based ethylene trimerization catalysts that can be activated with a stoichiometric amount of activator. The behavior of these activated, cationic complexes is distinct from the reaction of the neutral species in the presence of ethylene, in which 1-hexene is not formed, indicating that cationic complexes with non-coordinating anions are necessary for catalytic activity. We observe that these complexes are more sensitive to reaction conditions than the original bp system. The addition of diethyl ether to these catalysts dramatically improves their activities, lifetimes, and turnover numbers to 1-hexene. More experiments are needed to understand the exact nature of this "ether effect." In our systems and the bp system we observe catalyst decomposition, which often occurs via a process that is first-order in chromium.

Using these well-defined catalysts, we have been able to carry out some mechanistic studies. Stoichiometric protonation of the triphenyl complex in the presence of a 1:1 mixture of C_2H_4 and C_2D_4 gives a statistical mixture of 1-hexene isotopomers that supports the presence of metallacyclic intermediates in the catalytic trimerization of ethylene. Our report represents the first experimental study using an active catalyst to investigate the mechanism of 1-hexene formation for these chromium-based systems. Under trimerization conditions, chromium-phenyl bonds are cleaved by insertion of ethylene, followed by β-hydrogen elimination and reductive elimination processes to give a variety of phenyl-containing products. Further quantification of these products is necessary to learn the relative rates of these initiation reactions.

Experimental

General Considerations. All air- and moisture-sensitive compounds were manipulated using standard vacuum line, Schlenk, or cannula techniques or in a glove box under a nitrogen atmosphere, as described previously.[28] All

gases were purified by passage over MnO on vermiculite and activated molecular sieves. Ethereal solvents were stored over sodium benzophenone ketyl, hydrocarbon solvents were stored over titanocene,[29] and halogenated solvents were dried over calcium hydride. Solvents were also dried by the method of Grubbs.[30] Dichloromethane-d_2, and chloroform-*d* were purchased from Cambridge Isotopes and distilled from calcium hydride. $MeNH_3Cl$ was purchased from Aldrich and dried under vacuum at 100 °C for 24 hours. Other materials were used as received. CD_3I, anhydrous NEt_3, and anhydrous $MgBr_2$ were purchased from Aldrich. Methylaluminumoxane was purchased from Aldrich as a 10 weight % solution in toluene. $CrPh_3(THF)_3$ (**8**),[14,15] $(Me)N(PCl_2)_2$,[18] and (PNP-d_{12})$CrCl_3$ (**17**)[24] were prepared as previously described.

Instrumentation. Most ^1H, ^{13}C, ^{19}F, and ^{31}P NMR spectra were recorded on a Varian Mercury 300 spectrometer at 299.868 MHz, 75.409 MHz, 282.087 MHz, and 121.389 MHz, respectively, at room temperature unless indicated otherwise. Some ^1H and ^{13}C and all ^2H NMR spectra were recorded on a Varian INOVA 500 spectrometer at 499.852 MHz, 125.669 MHz, or 76.848 MHz, respectively, at room temperature unless indicated otherwise. All ^1H and ^{13}C NMR chemical shifts are reported relative to TMS, and ^1H (residual) or ^{13}C chemical shifts of the solvent are used as a secondary standard. ^{19}F NMR shifts are reported relative to an external $CFCl_3$ standard, and ^{31}P NMR shifts are reported relative to an external H_3PO_4 standard. ^2H NMR chemical shifts are reported with respect to $CHDCl_2$ (natural abundance, 5.32 ppm) from the CH_2Cl_2 solvent or to an external D_2O reference (4.8 ppm). Temperatures of the NMR probe were calibrated using a methanol standard. EPR spectra were recorded on a Bruker EMX spectrometer. Elemental analysis was performed by Midwest MicroLab, LLC. GC measurements were taken on an Agilent 6890 Series GC using an Agilent HP-5 column. X-ray crystallography was carried out by Dr. Michael W. Day and Lawrence M. Henling using an Enraf-Nonius CAD-4 diffractometer.

Synthesis of 2-Bromoanisole-d_3. In the glove box dry NaH (4.139 g, 172 mmol, 1.2 equiv) was placed in a 500 mL bomb. On the vacuum line approximately 250 mL of THF was added to the bomb via vacuum transfer. The bomb was placed on the Schlenk line, and 2-Bromophenol (16.6 mL, 143 mmol, 1 equiv) was added via syringe at 0 °C. Dihydrogen evolution was observed. After this reaction was allowed to warm to room temperature and stir for 2-3 hours, CD_3I (10.6 mL, 166 mmol, 1.2 equiv) was added via syringe. The bomb was sealed and protected from light, and the reaction was heated at 40 °C for 36 hours. The product was quenched with aqueous NH_4Cl and isolated by a basic aqueous workup to give 25.820 g of 2-bromoanisole-d_3 in 95.0% yield. The compound was dried over CaH_2 for 14 hours and distilled under full vacuum.

Synthesis of 2-Bromothioanisole-d_3. 2-Bromothiophenol (25.000 g, 132 mmol, 1 equiv) was placed in a 250 mL round bottom flask, and ethanol was added. Solid KOH (8.903 g, 159 mmol, 1.2 equiv) was added to the solution, and the mixture got warm and was allowed to stir for 1 hour. The flask was equipped with a rubber septum, the solution was cooled to 0 °C, and CD_3I (9.3 mL, 146 mmol, 1.1 equiv) was added via syringe. The solution was allowed to warm to room temperature and stirred overnight. The product was isolated by an aqueous workup to give 26.061 g of 2-bromothioanisole-d_3 in 95.7% yield. The compound was dried over CaH_2 for 14 hours and distilled under full vacuum.

Synthesis of PNP^{OMe}-d_{12} (9). *Route A.* In the glove box a Schlenk flask was charged with magnesium turnings (2.398 g, 99 mmol, 1.25 equiv) and equipped with a reflux condenser. Dry THF (100 mL) was added to the flask via vacuum transfer. Neat 2-bromoanisole-d_3 (15.000 g, 79 mmol, 1 equiv) was added slowly via syringe. A crystal of I_2 was added to initiate the Grignard reaction. The reaction was heated to 40 °C for 16 hours. The Grignard solution was added dropwise via cannula to a –78 °C solution of PBr_3 (3.75 mL, 39 mmol, 0.5 equiv) in 50 mL of THF in a Schlenk flask. The

solution was left to warm to room temperature and stir for 2 hours. The solution was again cooled to –78 °C, and solid $MeNH_3Cl$ (1.332 g, 20 mmol, 0.25 equiv) was added, followed by addition of anhydrous NEt_3 (10 mL, excess) via syringe. The reaction was allowed to warm to room temperature and stir for 16 hours. THF was removed *in vacuo*. Dry methanol was added via cannula to give a solution with white precipitate. The solution was filtered, and the solid was washed many times with methanol to remove salts. In air, 5 mL of dichloromethane were added to dissolve the white solid and 30 mL of methanol were added to precipitate out the product. The mixture was stored at –40 °C overnight and 5.277 g (50.3% yield) of white solid were collected by filtration of the cold solution. *Route B.* The Grignard reagent was prepared as described above using 3.720 g of magnesium (153 mmol, 1.3 equiv) and 2-bromoanisole-d_3 (15 mL, 119 mmol, 1 equiv). The solution of Grignard was cannula transferred into a THF solution of $(Me)N(PCl_2)_2$ (6.605 g, 28 mmol, 0.24 equiv). The reaction was stirred for 4 days, solvent was removed in vacuo, and 6.231 g of the product were isolated as described above in 39% yield. ^{1}H NMR (RT, 300 MHz, $CDCl_3$): δ = 2.44 (t, 3H, $Ar_2PN(CH_3)PAr_2$), 6.91 (t, 4H, Ar*H*), 6.99 (m, 4H, Ar*H*), 7.15 (m, 4H, Ar*H*), 7.37 (m, 4H, Ar*H*). ^{31}P NMR (RT, 300 MHz, $CDCl_3$): δ = 54 ppm (s, $Ar_2PN(Me)PAr_2$). ^{2}H NMR (RT, 500 MHz, CH_2Cl_2): δ = 3.60 ppm (s, OCD_3).

Synthesis of PNP^{SMe}-d_{12} (10). In the glove box a Schlenk flask was charged with magnesium turnings (1.474 g, 61 mmol, 1.24 equiv). On the vacuum line dry THF (100 mL) was added to the flask via vacuum transfer. Neat 2-bromothioanisole-d_3 (10.000 g, 49 mmol, 1 equiv) was added via syringe. The reaction mixture became warm upon addition and turned a pale brown color, and the reaction was left to stir at room temperature for 24 hours. The Grignard solution was cannula transferred to a THF solution of $(Me)N(PCl_2)_2$ (2.626 g, 11 mmol, 0.22 equiv), which causes the solution to get warm, and the resulting yellow solution is stirred at room temperature for 1 week. The product is isolated following the procedure used for isolation of **9** to obtain 1.598 g of **10** (22% yield). ^{1}H NMR (RT, 300 MHz, $CDCl_3$): δ = 2.51 (t, 3H,

$Ar_2PN(CH_3)PAr_2$), 7.06 (m, 8H, Ar*H*), 7.32 (m, 8H, Ar*H*). ^{31}P NMR (RT, 300 MHz, $CDCl_3$): δ = 50 ppm (s, $Ar_2PN(Me)PAr_2$). ^2H NMR (RT, 500 MHz, CH_2Cl_2): δ = 2.26 ppm (s, OCD_3).

Synthesis of (PNP^{OMe}-d_{12})$CrPh_3$ (11). In the glove box, compound **9** (1.069 g, 2.01 mmol, 1.03 equiv) was dissolved in 75 mL of dichloromethane. Portions of $CrPh_3(THF)_3$ (0.974 g, 1.95 mmol, total, 1 equiv) were added as a slurry in tetrahydrofuran (approximately 2 mL) to the stirring solution of **9** over 5 min. The color of the reaction mixture turned deep red upon addition. Volatile materials were removed *in vacuo*, approximately 50 mL of dichloromethane were added, followed by solvent removal *in vacuo*. The red solid residue was dissolved in approximately 25 mL of dichloromethane and approximately 30 mL of petroleum ether were added to precipitate a red solid. This mixture was stored at –35 °C overnight. The solid material collected by filtration of the cold solution was recrystallized from a dichloromethane/petroleum ether mixture, collected on a sintered glass frit, and dried under vacuum to leave 1.050 g of **11** as a red, microcrystalline solid (68% yield). ^2H NMR (RT, 500 MHz, CH_2Cl_2): δ = 8.47 ppm (s, OCD_3). Anal. Calcd for $C_{47}H_{34}D_{12}NO_4P_2Cr$: C, 69.26; H, 5.70; N, 1.72. Found: C, 69.03; H, 5.69; N, 1.86. $\mu_{eff} = 3.8\ \mu_B$. X-ray quality crystals of **11** were obtained from slow diffusion of petroleum ether into a concentrated CH_2Cl_2 solution of the complex at –35 °C.

Synthesis of (PNP^{SMe}-d_{12})$CrPh_3$ (12). Compound **12** was prepared using an analogous procedure to that used for compound **11** from **10** (1.252 g, 2.10 mmol, 1 equiv) and **8** (1.050 g, 2.10 mmol, 1 equiv). An orange-brown solid is obtained, which is taken up in approximately 25 mL of dichoromethane and approximately 25 mL of petroleum ether were added to precipitate a brown solid. This mixture was stored at –35 °C overnight. The solid material collected by filtration of the cold solution was recrystallized from a dichloromethane/petroleum ether mixture, collected on a sintered glass frit, and dried under vacuum to leave 1.039 g of **12** as a brown solid (56% yield). ^2H NMR (RT, 500 MHz, CH_2Cl_2): δ = -3.8 ppm (s, SCD_3). Anal. Calcd for

$C_{47}H_{34}D_{12}NS_4P_2Cr$: C, 65.09; H, 5.36; N, 1.62. Found: C, 64.83; H, 5.35; N, 1.72. X-ray quality crystals of **12** were obtained from slow diffusion of petroleum ether into a concentrated CH_2Cl_2 solution of the complex at –35 °C.

Synthesis of (PNP^{OMe}-d_{12})$CrPh_2X$ (13). In the glovebox, solid **11** (0.089 g, 0.109 mmol, 1 equiv) and $MgBr_2$ (0.037 g, 0.201 mmol, 1.8 equiv) are placed in a 20 mL vial. Approximately 3 mL of dichloromethane were added to form a red solution with white precipitate (presumably insoluble $MgBr_2$). The reaction is stirred at room temperature, and within 24 hours the solution is brown. After 41 hours the solution is dark green. The solution is filtered to remove a white solid and leave a dark green solution. Approximately 2 mL of petroleum ether were added to the filtrate to precipitate some white and brown solids, which were removed by filtration. Again approximately 2 mL of petroleum ether were added to this filtrate to precipitate more white and brown solids, which were removed by filtration. To this filtrate were added approximately 2 mL of petroleum ether, and the solution was stored at –35 °C overnight. The dark green crystals collected by filtration of the cold solution were used to obtain an X-ray structure of this complex, which can be modeled as a 3:1 mixture of (PNP^{OMe}-d_{12})$CrPh_2Cl$ and (PNP^{OMe}-d_{12})$CrPh_2Br$. ^2H NMR (RT, 500 MHz, CH_2Cl_2): δ = 6 ppm (br s, OCD_3).

Synthesis of (PNP^{OMe}-d_{12})$CrPh_2Cl$ (14). In the glovebox, solid **11** (0.517 g, 0.63 mmol, 2 equiv) and solid **17** (0.219 g, 0.32 mmol, 1 equiv) were placed in a 20 mL vial. Approximately 10 mL of CH_2Cl_2 were added to form a brown solution. The vial was wrapped in aluminum foil to protect it from light, and the reaction was allowed to stir at room temperature for 2 hours. The mixture turned a dark green color. Solvent was removed *in vacuo* to leave a green-brown powder, which was dissolved in approximately 10 mL of dichloromethane and approximately 7 mL of petroleum ether were added to precipitate a green-brown solid. This mixture was stored at –35 °C overnight. The solid material collected by filtration of the cold solution was recrystallized from a dichloromethane/petroleum ether mixture, collected on

a sintered glass frit, and dried under vacuum to leave 0.523 g of **14** as a green-brown powder (71% yield). ^{2}H NMR (RT, 500 MHz, CH_2Cl_2): δ = 6 ppm (br s, OC*D*$_3$). Anal. Calcd for $C_{41}H_{29}D_{12}ClNO_4P_2Cr$: C, 64.69; H, 5.44; N, 1.84. Found: C, 64.87; H, 6.06; N, 1.65. X-ray quality crystals of **14** were obtained from slow diffusion of petroleum ether into a concentrated chlorobenzene solution of the complex at –35 °C.

Synthesis of [(PNP^{OMe}-*d*$_{12}$)CrPhCl]$_2^{2+}$/2 AlCl$_4^-$ (15). Solid **11** (0.036 g, 0.044 mmol, 1 equiv) and $AlCl_3$ (0.010 g, 0.075 mmol, 1.7 equiv) were placed in a 20 mL vial in the glovebox. Dichloromethane (5 mL) was added and the mixture turned a bright green color. Diethyl ether (8 mL) was added and the mixture was cooled to –35 °C for 6 days, at which point some bright turquoise crystals were observed to have formed in the vial. These crystals were identified by X-ray crystallography.

Synthesis of (PNP^{OMe}-*d*$_{12}$)CrPhCl$_2$ (18). Solid **11** (0.014 g, 0.017 mmol, 1 equiv) and solid **17** (0.024 g, 0.035 mmol, 2 equiv) were placed in a 20 mL vial and approximately 2 mL of dichloromethane were added. The mixture was wrapped in aluminum foil to protect it from light and left to stir at room temperature for 12 hours. The solution turned a dark green color. ^{2}H NMR (RT, 500 MHz, CH_2Cl_2): δ = 4.4 ppm (s, 6D, OC*D*$_3$), 11.8 ppm (s, 6D, OC*D*$_3$).

Variable temperature ^{2}H NMR study of 11, 12, 14, and 18. The experiments were performed in CH_2Cl_2 or PhCl solutions. At high temperatures (fast exchange) the spectra showed one peak. Upon cooling down two decoalescence processes were observed. The higher temperature one splits the peak to two peaks (one broad peak found between 10-20 ppm and one sharp peak found in the diamagnetic region at approximately 3-4 ppm) in a 1:1 ratio. The lower temperature decoalescence splits the broad peak mentioned above into two peaks – one broad and shifted downfield (> 20 ppm) and one in the diamagnetic region (overlapping with the other diamagnetic peaks).

General procedure for trimerization of C_2H_4 with 11/$H^+(Et_2O)_2B[C_6H_3(CF_3)_2]_4^-$. In the glove box a 250 mL round bottom flask was charged with **11** (0.016 g, 0.020 mmol, 1 equiv) and $H^+(Et_2O)_2B[C_6H_3(CF_3)_2]_4^-$ (0.020 g, 0.020 mmol, 1 equiv), and approximately 2 mL of diethyl ether was added, followed by 48 mL of toluene to give a pale green solution. The flask was equipped with a 180 ° needle valve, degassed on the vacuum line at –78 °C, warmed to room temperature, and backfilled with 1 atmosphere of ethylene. Ethylene consumption was monitored using a mercury manometer. After 1 h the reaction was quenched with H_2O. The organic fraction was separated and filtered through a plug of activated alumina to remove any chromium, and this mixture was analyzed by GC and GC-MS. 1-Hexene was quantified by comparison to a mesitylene standard, which was added to the reaction mixture. The reaction produces 1-hexene with a range of 700 – 3,000 turnovers in greater than 85% overall selectivity. A similar procedure was followed in the case of activation of **11** with $Me_2PhNH^+B[C_6F_5]_4^-$ or MAO.

General procedure for trimerization of C_2H_4 with 14/$Na^+B[C_6H_3(CF_3)_2]_4^-$. In the glove box a 250 mL round bottom flask was charged with **14** (0.017 g, 0.022 mmol, 1 equiv) and $Na^+B[C_6H_3(CF_3)_2]_4^-$ (0.021 g, 0.024 mmol, 1.1 equiv) and equipped with a 180 ° needle valve. The flask was attached to the vacuum line and approximately 50 mL of chlorobenzene were added via vacuum transfer. The flask was backfilled with 1 atmosphere of ethylene, and the mixture was allowed to warm to room temperature and stir while open to an ethylene atmosphere. A pale green solution was formed as the mixture melted, and the reaction was stirred for 20 minutes to 1.5 hours, at which point it was quenched with H_2O. The organic fraction was separated and filtered through a plug of activated alumina to remove any chromium, and this mixture was analyzed by GC and GC-MS. The reaction produces 1-hexene with a range of 300 – 1,000 turnovers in greater than 85% overall selectivity.

General procedure for trimerization of C_2H_4 with $CrCl_3(THF)_3$/PNP/ MAO. In the glove box a 250 mL round bottom flask was charged with **9** (0.011 g, 0.021 mmol, 1 equiv) and $CrCl_3(THF)_3$ (0.008 g, 0.021 mmol, 1 equiv), 50 mL of toluene were added, and the flask was equipped with a 180 ° needle valve. The apparatus was attached to the high vacuum line, degassed at –78 ° C, and backfilled with 1 atmosphere of ethylene. After the solution had warmed to room temperature, MAO solution (3.481 g, 10 weight % in toluene, 6 mmol, 300 equiv) was added via syringe under a positive ethylene flow. Ethylene consumption was monitored using a mercury manometer. After 1 h the reaction was quenched with H_2O. The organic fraction was separated and filtered through a plug of activated alumina to remove any chromium, and this mixture was analyzed by GC and GC-MS. The reaction produces 1-hexene with a range of 1,000-4,700 turnovers in greater than 85% overall selectivity.

Trimerization of a C_2D_4/C_2H_4 mixture with 11/$H^+(Et_2O)_2B[C_6H_3(CF_3)_2]_4^-$. Chlorobenzene was vacuum transferred into a Schlenk tube charged with **11** (0.018 g, 0.022 mmol, 1 equiv) and $H^+(Et_2O)_2B[C_6H_3(CF_3)_2]_4^-$ (0.022 g, 0.022 mmol, 1 equiv). A 1:1 mixture of C_2D_4 and C_2H_4 (128.2 mL at 213 torr, 1480 mmol, 67 equiv) was condensed into the tube at –192 °C (approximately 1.8 atm at room temperature). The reaction mixture was allowed to warm to room temperature and left to stir during which time the mixture changed from a red-brown color to a green-brown color. After stirring for 1.5 hours at room temperature, the reaction was vented and quenched with H_2O. The organic fraction was separated and filtered through a plug of activated alumina to remove any chromium, and this mixture was analyzed by GC-MS. The 1-hexene fraction resolves in a quartet showing a 1:3:3:1 distribution of isotopomers (C_6H_{12}, $C_6H_8D_4$, $C_6H_4D_8$, and C_6D_{12}).

Crystallography. Crystal data, intensity collection, and refinement details are presented in Tables 4-7 for compounds **11**, **13**, **14**, and **15**.

Data Collection and Processing. Data for compounds **11**, **13**, **14**, and **15** were collected on a Bruker SMART 1000 running SMART.[31] The diffractometer was equipped with a Crystal Logic CL24 low temperature device, and all data sets were collected at 98 K. The diffractometer used graphite-monochromated MoKα radiation with λ = 0.71073 Å. The crystals were mounted on a glass fiber with Paratone-N oil. Data were collected as ω-scans at 3 to 7 ϕ settings. The detector was 5 cm (nominal) distant at a θ angle of -28°. The data were processed with SAINT.[31]

Empirical Formula	$C_{47}H_{46}NO_4P_2Cr \bullet 3\ CH_2Cl_2$
Formula Weight (g/mol)	1057.57
Crystallization Solvent	Dichloromethane/Petroleum Ether
Crystal Habit	Block
Crystal Size (mm^3)	0.26 X 0.17 X 0.11
Crystal Color	Dark Red
Preliminary Photos	Rotation
Type of Diffractometer	Bruker SMART 1000
Wavelength	0.71073 Å MoKα
Data Collection Temperature (K)	98(2)
θ Range for 23120 Reflections Used in Lattice Determination (°)	2.20 to 27.69
Unit Cell Dimension a (Å)	15.1624(7)
Unit Cell Dimension b (Å)	15.4024(7)
Unit Cell Dimension c (Å)	22.7168(11)
α (°)	91.2320(10)
β (°)	94.4350(10)
γ (°)	110.5250(10)
Volume ($Å^3$)	4946.8(4)
Z	4
Crystal System	Triclinic
Space Group	P^{-1}
Calculated Density (Mg/m^3)	1.420
F(000)	2188
Data Collection Program	Bruker SMART
θ Range for Data Collection (°)	1.41 to 28.46
Completeness to θ = 28.46° (%)	91.7
Index Ranges	$-20 \le h \le 20$, $-20 \le k \le 20$, $-30 \le l \le 29$
Data Collection Scan Type	ω scans at 7 ϕ settings
Data Reduction Program	Bruker SAINT v6.2
Reflections Collected	102,892
Independent Reflections	22,906 (R_{int} = 0.0806)
Absorption Coefficient (mm^{-1})	0.665

Absorption Correction	None
Max. and Min. Transmission (Calculated)	0.9304 and 0.8461
Structure Solution Program	SHELXS-97 (Sheldrick, 1990)
Primary Solution Method	Direct Methods
Secondary Solution Method	Difference Fourier Map
Hydrogen Placement	Geometric Positions
Structure Refinement Program	SHELXL-97 (Sheldrick, 1997)
Refinement method	Full matrix least-squares on F^2
Data/Restraints/Paramaters	22906/0/1138
Treatment of Hydrogen Atoms	Constrained
Goodness-of-Fit[a] on F^2	2.003
Final R Indices[b] (I > 2s(I), 14122 Reflections)	R1 = 0.0692, *w*R2 = 0.1163
R Indices[b] (All Data)	R1 = 0.1196, *w*R2 = 0.1216
Type of Weighting Scheme Used	Sigma
Weighting Scheme Used	$w = 1/\sigma^2(Fo^2)$
Max Shift/Error	0.004
Average Shift/Error	0.000
Largest Diff. Peak and Hole (e/Å^3)	2.556 and –1.427

Table 4. X-ray experimental data for **11**. [a]Goodness-of-Fit (S) is based on F^2; F set to zero for negative F^2. [b]R-factors (R) are based on F and weighted R-factors (*w*R) are based on F^2.

Empirical Formula	$C_{41}H_{41}NO_4P_2Br_{0.24}Cl_{0.76}Cr \bullet 2 CH_2Cl_2$
Formula Weight (g/mol)	942.10
Crystallization Solvent	Dichloromethane/Petroleum Ether
Crystal Habit	Block
Crystal Size (mm^3)	0.18 X 0.12 X 0.07
Crystal Color	Dark Green
Preliminary Photos	Rotation
Type of Diffractometer	Bruker SMART 1000
Wavelength	0.71073 Å MoKα
Data Collection Temperature (K)	98(2)
θ Range for 6715 Reflections Used in Lattice Determination (°)	2.21 to 27.20
Unit Cell Dimension a (Å)	11.8927(8)
Unit Cell Dimension b (Å)	18.3553(13)
Unit Cell Dimension c (Å)	19.4610(13)
Volume (Å^3)	4248.2(5)
Z	4
Crystal System	Orthorhombic
Space Group	$P2_12_12_1$
Calculated Density (Mg/m^3)	1.473
F(000)	1942

Data Collection Program	Bruker SMART
θ Range for Data Collection (°)	1.53 to 28.57
Completeness to θ = 28.57° (%)	93.2
Index Ranges	$-15 \le h \le 8$, $-23 \le k \le 23$, $-25 \le l \le 23$
Data Collection Scan Type	ω scans at 3 ϕ settings
Data Reduction Program	Bruker SAINT v6.2
Reflections Collected	26,610
Independent Reflections	9,791 (R_{int} = 0.0744)
Absorption Coefficient (mm^{-1})	0.922
Absorption Correction	None
Max. and Min. Transmission (Calculated)	0.9349 and 0.8516
Structure Solution Program	SHELXS-97 (Sheldrick, 1990)
Primary Solution Method	Direct Methods
Secondary Solution Method	Difference Fourier Map
Hydrogen Placement	Geometric Positions
Structure Refinement Program	SHELXL-97 (Sheldrick, 1997)
Refinement method	Full matrix least-squares on F^2
Data/Restraints/Paramaters	9791/6/520
Treatment of Hydrogen Atoms	Riding
Goodness-of-Fit[a] on F^2	1.065
Final R Indices[b] (I > 2s(I), 6804 Reflections)	R1 = 0.0474, *w*R2 = 0.0765
R Indices[b] (All Data)	R1 = 0.0815, *w*R2 = 0.0834
Type of Weighting Scheme Used	Sigma
Weighting Scheme Used	$w = 1/\sigma^2(Fo^2)$
Max Shift/Error	0.001
Average Shift/Error	0.000
Absolute Structure Parameter	-0.002(19)
Largest Diff. Peak and Hole (e/Å^3)	2.556 and –1.427

Table 5. X-ray experimental data for **13**. [a]Goodness-of-Fit (S) is based on F^2; F set to zero for negative F^2. [b]R-factors (R) are based on F and weighted R-factors (*w*R) are based on F^2.

Empirical Formula	$C_{41}H_{41}NO_4P_2Cr \bullet 0.5\ C_6H_5Cl$
Formula Weight (g/mol)	799.69
Crystallization Solvent	Chlorobenzene/Petroleum Ether
Crystal Habit	Thin Hexagon
Crystal Size (mm^3)	0.33 X 0.24 X 0.07
Crystal Color	Dichroic Green/Brown
Preliminary Photos	Rotation
Type of Diffractometer	Bruker SMART 1000
Wavelength	0.71073 Å MoKα
Data Collection Temperature (K)	98(2)

θ Range for 11713 Reflections Used in Lattice Determination (°)	2.19 to 32.17
Unit Cell Dimension a (Å)	10.5083(6)
Unit Cell Dimension b (Å)	11.2424(7)
Unit Cell Dimension c (Å)	18.3603(10)
α (°)	93.9640(10)
β (°)	92.9940(10)
γ (°)	115.0850(10)
Volume ($Å^3$)	1951.8(2)
Z	2
Crystal System	Triclinic
Space Group	P^{-1}
Calculated Density (Mg/m^3)	1.361
F(000)	835
Data Collection Program	Bruker SMART v5.054
θ Range for Data Collection (°)	2.01 to 32.75
Completeness to θ = 32.75° (%)	83.2
Index Ranges	$-15 \le h \le 15$, $-14 \le k \le 16$, $-27 \le l \le 27$
Data Collection Scan Type	ω scans at 5 ϕ settings
Data Reduction Program	Bruker SAINT v6.45
Reflections Collected	32,181
Independent Reflections	11,984 (R_{int} = 0.0704)
Absorption Coefficient (mm^{-1})	0.488
Absorption Correction	None
Max. and Min. Transmission (Calculated)	0.9667 and 0.8556
Structure Solution Program	SHELXS-97 (Sheldrick, 1990)
Primary Solution Method	Direct Methods
Secondary Solution Method	Difference Fourier Map
Hydrogen Placement	Geometric Positions
Structure Refinement Program	SHELXL-97 (Sheldrick, 1997)
Refinement method	Full matrix least-squares on F^2
Data/Restraints/Paramaters	11984/0/507
Treatment of Hydrogen Atoms	Riding
Goodness-of-Fit[a] on F^2	1.472
Final R Indices[b] (I > 2s(I), 7848 Reflections)	R1 = 0.0509, *w*R2 = 0.0985
R Indices[b] (All Data)	R1 = 0.0836, *w*R2 = 0.1030
Type of Weighting Scheme Used	Sigma
Weighting Scheme Used	$w = 1/\sigma^2(Fo^2)$
Max Shift/Error	0.005
Average Shift/Error	0.000
Largest Diff. Peak and Hole ($e/Å^3$)	1.071 and –0.562

Table 6. X-ray experimental data for **14**. [a]Goodness-of-Fit (S) is based on F^2; F set to zero for negative F^2. [b]R-factors (R) are based on F and weighted R-factors (*w*R) are based on F^2.

Empirical Formula	$[C_{70}H_{72}N_2O_8P_4Cr_2]^{2+}2[AlCl_4]^- \bullet 2 CH_2Cl_2 \bullet C_5H_{12}$
Formula Weight (g/mol)	1947.63
Crystallization Solvent	Dichloromethane/Petroleum Ether
Crystal Habit	Plate
Crystal Size (mm^3)	0.35 X 0.26 X 0.09
Crystal Color	Emerald Green
Preliminary Photos	Rotation
Type of Diffractometer	Bruker SMART 1000
Wavelength	0.71073 Å MoKα
Data Collection Temperature (K)	98(2)
θ Range for 15255 Reflections Used in Lattice Determination (°)	4.26 to 24.75
Unit Cell Dimension a (Å)	13.6289(14)
Unit Cell Dimension b (Å)	26.434(3)
Unit Cell Dimension c (Å)	24.738(2)
β (°)	101.1380(10)
Volume ($Å^3$)	8744.4(15)
Z	4
Crystal System	Monoclinic
Space Group	$P2_1/c$
Calculated Density (Mg/m^3)	1.479
F(000)	4000
Data Collection Program	Bruker SMART v5.054
θ Range for Data Collection (°)	4.24 to 25.22
Completeness to θ = 25.22° (%)	92.5
Index Ranges	$-16 \le h \le 16, -30 \le k \le 31, -29 \le l \le 29$
Data Collection Scan Type	ω scans at 5 ϕ settings
Data Reduction Program	Bruker SAINT v6.45
Reflections Collected	80,952
Independent Reflections	14,623 (R_{int} = 0.1042)
Absorption Coefficient (mm^{-1})	0.823
Absorption Correction	None
Max. and Min. Transmission (Calculated)	0.9296 and 0.7616
Structure Solution Program	SHELXS-97 (Sheldrick, 1990)
Primary Solution Method	Direct Methods
Secondary Solution Method	Difference Fourier Map
Hydrogen Placement	Difference Fourier Map
Structure Refinement Program	SHELXL-97 (Sheldrick, 1997)
Refinement method	Full matrix least-squares on F^2
Data/Restraints/Paramaters	14623/89/982
Treatment of Hydrogen Atoms	Unrestrained
Goodness-of-Fit[a] on F^2	2.153
Final R Indices[b] (I > 2s(I), 8075 Reflections)	R1 = 0.0734, *w*R2 = 0.1282
R Indices[b] (All Data)	R1 = 0.1446, *w*R2 = 0.1357

Type of Weighting Scheme Used	Sigma
Weighting Scheme Used	$w = 1/\sigma^2(Fo^2)$
Max Shift/Error	0.010
Average Shift/Error	0.000
Largest Diff. Peak and Hole (e/Å^3)	3.082 and –2.586

Table 7. X-ray experimental data for **15**. [a]Goodness-of-Fit (S) is based on F^2; F set to zero for negative F^2. [b]R-factors (R) are based on F and weighted R-factors (*w*R) are based on F^2.

Structure Analysis and Refinement. Crystallographic data for the structure of **11** (CCDC 216617) have been deposited with the Cambridge Crystallographic Data Centre (CCDC), 12 Union Road, Cambridge CB2, 1EZ, UK, and copies can be obtained on request, free of charge, by quoting the deposition number 216617. Structure factors are available electronically by e-mail: xray@caltech.edu. Crystallographic data for the structure of **13** (CCDC 208717) have been deposited with the Cambridge Crystallographic Data Centre (CCDC), 12 Union Road, Cambridge CB2, 1EZ, UK, and copies can be obtained on request, free of charge, by quoting the deposition number 208717. Structure factors are available electronically by e-mail: xray@caltech.edu. Crystallographic data for the structure of **14** (CCDC 228269) have been deposited with the Cambridge Crystallographic Data Centre (CCDC), 12 Union Road, Cambridge CB2, 1EZ, UK, and copies can be obtained on request, free of charge, by quoting the deposition number 228269. Structure factors are available electronically by e-mail: xray@caltech.edu. Crystallographic data for the structure of **15** (CCDC 232041) have been deposited with the Cambridge Crystallographic Data Centre (CCDC), 12 Union Road, Cambridge CB2, 1EZ, UK, and copies can be obtained on request, free of charge, by quoting the deposition number 232041. Structure factors are available electronically by e-mail: xray@caltech.edu.

References

[1] (a) Skupinska, J. *Chem. Rev.* **1991**, *91*, 613. (b) Keim, W.; Kowaldt, F. H.; Goddard, R.; Krüger, C. *Angew. Chem., Int. Ed. Engl.* **1978**, *17*, 466. (c) Svejda, S. A.; Brookhart, M. *Organometallics* **1999**, *18*, 65. (d) Killian, C. M.; Johnson, L. K.; Brookhart, M. *Organometallics* **1997**, *16*, 2005. (e) Mecking, S. *Coord. Chem. Rev.* **2000**, *203*, 325. (f) Ruther, T.; Braussaud, N.; Cavell, K. J. *Organometallics* **2001**, *20*, 1247. (g) Britovsek, G. J. P.; Mastroianni, S.; Solan, G. A.; Baugh, S. P. D.; Redshaw, C.; Gibson, V. C.; White, A. J. P.; Williams, D. J.; Elsegood, M. R. J. *Chem. Eur. J.* **2000**, *6*, 2221.

[2] Vogt, D. in *Applied Homogeneous Catalysis with Organometallic Compounds*; Cornils, B., Herrmann, W. A., Eds.; VCH: Weinheim, Germany, 1996.

[3] Briggs, J. R. *J. Chem. Soc., Chem. Commun.* **1989**, 674.

[4] (a) Kohn, R. D.; Haufe, M.; Kociok-Kohn, G.; Grimm, S.; Wasserscheid, P.; Keim, W. *Angew. Chem., Int. Ed.* **2000**, *39*, 4337. (b) Reagen, W. K.; Pettijohn, T. M.; Freeman, J. W. (Philips Petroleum Co.). Patent US 5,523,507, 1996. (c) McGuinness, D. S.; Wasserscheid, P.; Keim, W.; Hu, C.; Englert, U.; Dixon, J. T.; Grove, C. *Chem. Commun.* **2003**, 334. (d) McGuinness, D. S.; Wasserscheid, P.; Keim, W.; Morgan, D.; Dixon, J. T.; Bollmann, A.; Maumela, H.; Hess, F.; Englert, U. *J. Am. Chem. Soc.* **2003**, *125*, 5272. (e) Wu, F.-J. (Amoco Corp.). Patent US 5,811,618, 1998.

[5] (a) Deckers, P. J. W.; Hessen, B.; Teuben, J. H. *Angew Chem., Int. Ed.* **2001**, *40*, 2516. (b) Deckers, P. J. W.; Hessen, B.; Teuben, J. H. *Organometallics* **2002**, *21*, 5122. (c) Pellechia, C.; Pappalardo, D.; Oliva, L.; Mazzeo, M.; Gruter, G.-J. *Macromolecules* **2000**, *33*, 2807.

[6] Andes, C.; Harkins, S. B.; Murtuza, S.; Oyler, K.; Sen, A. *J. Am. Chem. Soc.* **2001**, *123*, 7423.

[7] Santi, R.; Romano, A. M.; Grande, M.; Sommazzi, A.; Masi, F.; Proto, A. (ENICHEM S.P.A.). WO 0168572, 2001.

[8] Cr(II) has also been shown to be active. See reference 9.

[9] (a) Carter, A.; Cohen, S. A.; Cooley, N. A.; Murphy, A.; Scutt, J.; Wass, D. F. *Chem. Commun.* **2002**, 858. (b) Wass, D. F. (British Petroleum). Patent WO 2002004119, 2002.

[10] Elowe, P. R.; Bercaw, J. E. Unpublished results.

[11] Janse van Rensburg, W.; Grové, C.; Steynberg, J. P. Stark, K. B.; Huyser, J. J.; Steynberg, P. J. *Organometallics* **2004**, *23*, 1207.

[12] (a) McDermott, J. X.; White, J. F.; Whitesides, G. M. *J. Am. Chem. Soc.* **1973**, *95*, 4451. (b) McDermott, J. X.; White, J. F.; Whitesides, G. M. *J. Am. Chem. Soc.* **1976**, *98*, 6521.

[13] Emrich, R.; Heinemann, O.; Jolly, P. W.; Krüger, C.; Verhovnik, G. P. J. *Organometallics* **1997**, *16*, 1511.

[14] Herwig, W.; Zeiss, H. *J. Am. Chem. Soc.* **1959**, *81*, 4798.

[15] Khan, S. I.; Bau, R. *Organometallics* **1983**, *2*, 1896.

[16] La Mar, G. N.; Horrocks, W. D., Jr.; Holm, R. H. *NMR of Paramagnetic Molecules*; Academic Press: New York, 1973.

[17] (a) Dossett, S. J.; Gillon, A.; Orpen, A. G.; Fleming, J. S.; Pringle, P. G.; Wass, D. F.; Jones, M. D. *Chem. Commun.* **2001**, 699. (b) Balakrishna, M. S.; Sreenivasa Reddy, V.; Krishnamurthy, S. S.; Nixon, J. F.; Burkett St. Laurent, J. C. T. R. *Coord. Chem. Rev.* **1994**, *129*, 1.

[18] King, R. B.; Gimeno, J. *Inorg. Chem.* **1978**, *17*, 2390.

[19] Drago, R. S. *Physical Methods in Chemistry*; W. B. Saunders Company: Philadelphia, 1977; Chs. 11-12.

[20] Bonomo, R. P.; Di Bilio, A. J.; Riggi, F. *Chem. Phys.* **1991**, *151*, 323.

[21] (a) Sur, S. K. *J. Magn. Reson.* **1989**, *82*, 169. (b) Evans, D. F. *J. Chem. Soc.* **1959**, 2003. (c) Schubert, E. M. *J. Chem. Educ.* **1992**, *69*, 62.

[22] Agapie, T.; Bercaw, J. E. Unpublished results.

[23] Klamo, S. B.; Bercaw, J. E. Unpublished results.

[24] Agapie, T.; Schofer, S. J.; Labinger, J. A.; Bercaw, J. E. *J. Am. Chem. Soc.* **2004**, *126*, 1304.

[25] Private communication with Angelo J. Di Bilio.

[26] Agapie, T.; Elowe, P. R.; Bercaw, J. E. Unpublished results.

[27] Emrich, R.; Heinemann, O.; Jolly, P. W.; Krüger, C.; Verhovnik, G. P. J. *Organometallics* **1997**, *16*, 1511.

[28] Burger, B.J.; Bercaw, J.E. in *Experimental Organometallic Chemistry*; ACS Symposium Series No. 357; Wayda, A.L.; Darensbourg, M.Y. Eds.; American Chemical Society: Washington, D.C. 1987; Ch. 4.

[29] Marvich, R.H.; Brintzinger, H.H. *J. Am. Chem. Soc.* **1971**, *93*, 203.

[30] Pangborn, A. B.; Giardello, M. A.; Grubbs, R. H.; Rosen, R. K.; Timmers, F. J. *Organometallics* **1996**, *15*, 1518.

[31] Bruker (1999) SMART, SAINT, and SHELXTL. Bruker AXS Inc., Madison, Wisconsin, USA.